Jets and Radio Loud AGN

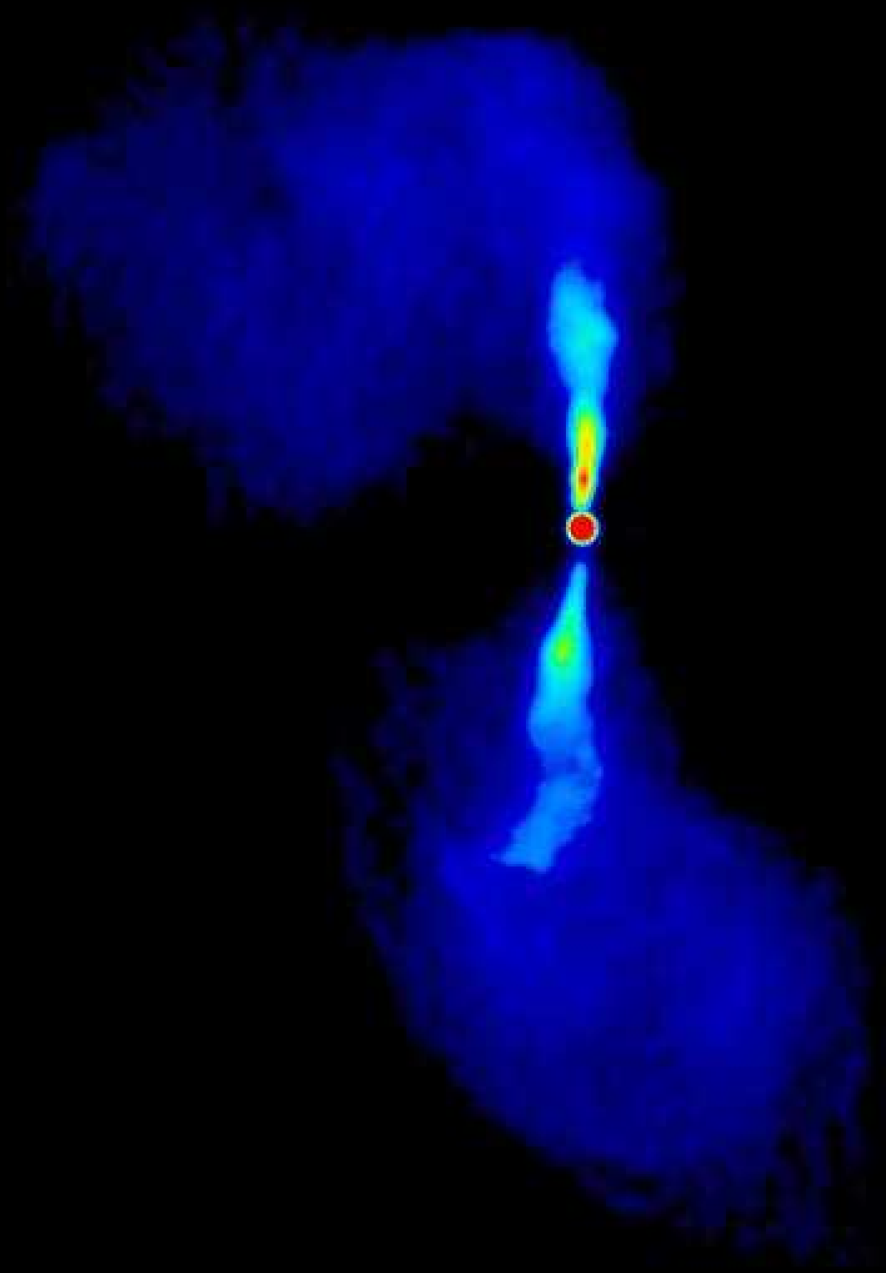

Fanaroff-Riley Type 1: strong nucleus, asymmetric jets with wide opening angle ending in plumes

M84 (3C272.1) (Laing & Bridle, 1987): VLA 4885 MHz, $134'' \times 170''$; see also
`http://www.jb.man.ac.uk/atlas/other/3C272P1`

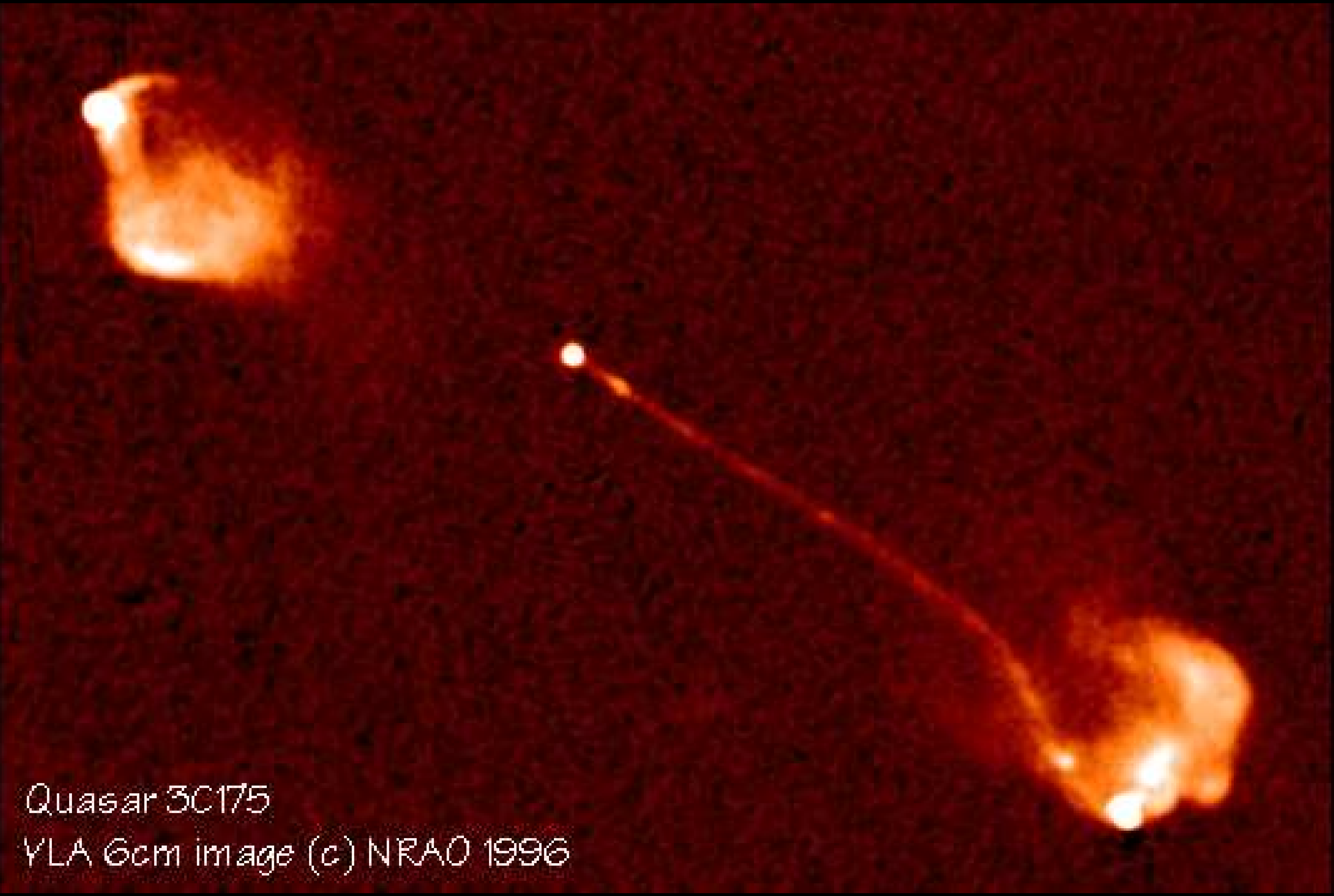

Radio image of 3C175 ($z = 0.768$; A. Bridle, priv. comm.)

Fanaroff-Riley Type 2: weak (one-sided) jet ending in radio lobes, lobe dominated

Synchrotron Radiation

Jets are observed to have strong polarization and power law radio spectrum. These are characteristics of synchrotron radiation.

Synchrotron-Radiation (=Magnetobremsstrahlung): Radiation emitted by relativistic electrons in a magnetic field.

Goal: Qualitative analysis:

1. Derive the motion of electrons in magnetic fields
2. Then use Larmor's formula to obtain the radiation characteristic from relativistic motion
3. Use the Doppler-effect to convert into the observer's frame of reference.
4. Integrate over electron distribution to obtain the final spectrum.

Detailed theory: see Ginzburg & Syrovatskii (1965), Ginzburg & Syrovatskii (1969), Blumenthal & Gould (1970), Reynolds (1982).

Relativistic Motion

Lorentz-Force ($\mathbf{E} = 0$)

$$\frac{d\mathbf{p}}{dt} = \frac{e}{c}\mathbf{v} \times \mathbf{B} \quad \text{where} \quad \mathbf{p} = \frac{m_\mathrm{e}\mathbf{v}}{\sqrt{1-\beta^2}} = \gamma m_\mathrm{e}\mathbf{v} \tag{10.1}$$

where $\beta = v/c$.

Assumption: No radiative losses (i.e., electron does *not* emit synchrotron radiation...): $\gamma =$ const.

Velocity-vector of the electron:

$$\mathbf{v}_{\|} = \frac{\mathbf{v}\cdot\mathbf{B}}{B}\frac{\mathbf{B}}{B} \qquad \mathbf{v}_{\perp} = \frac{\mathbf{B}\times(\mathbf{v}\times\mathbf{B})}{B^2} \tag{10.2}$$

$$|\mathbf{v}_{\|}| = v\cos\alpha \qquad |\mathbf{v}_{\perp}| = v\sin\alpha \tag{10.3}$$

where α (pitch-angle): $\angle(\mathbf{v},\mathbf{B})$

No acceleration parallel to the $\mathbf{B}$-fi eld $\Longrightarrow$ only $v_\perp$ is interesting $\Longrightarrow$ circular motion:

$$m_\mathrm{e}a_\perp = \frac{\gamma m_\mathrm{e} v_\perp^2}{R} = \frac{e}{c}\mathrm{v}_\perp B \tag{10.4}$$

$$\frac{v_\perp}{R} = \frac{eB}{\gamma m_\mathrm{e} c} = \frac{\omega_\mathrm{L}}{\gamma} = \omega_\mathrm{B} \tag{10.5}$$

where $\omega_\mathrm{L} = 2\pi\nu_\mathrm{L}$: Larmor frequency (also Cyclotron frequency, gyrofrequency).

Numerical values

Numerically, Larmor frequency is

$$\nu_{\mathrm{L}} = 2.8 B_{1\,\mathrm{G}}\,\text{MHz} \tag{10.6}$$

The radius of the orbit (Larmor radius) is

$$R = \frac{\gamma v_{\perp}}{\omega_{\mathrm{L}}} \approx 10^7 \frac{E_{1\mathrm{GeV}}}{B_{1\,\mathrm{G}}}\,\text{cm} \tag{10.7}$$

Typical values:

$$\boxed{B \approx 10^{-5}\,\text{G},\ E = 1\,\text{GeV},\ \Longrightarrow R = 3 \times 10^{13}\,\text{cm (2 AU).}}$$

i.e., small on cosmic scales

Radiated Energy, I

Electrodynamics: Radiation of an accelerated electron:

$$P_{\mathrm{em}} = \frac{2e^2}{3c^3}\gamma^4\left(a_\perp^2 + \gamma^2 a_\parallel^2\right) \tag{10.8}$$

where a is the acceleration.

([Messy] derivation by Lorentz-transforming the classical Larmor formula ($P = (2e^2/3c^3) \cdot a^3$), see, e.g., Shu)

For circular motion, $a_\perp = \omega_\mathrm{B}\mathrm{v}_\perp$ and $a_\parallel = 0$. Hence

$$P_{\mathrm{em}} = \frac{2e^2}{3c^3}\gamma^4\frac{v_\perp^2 e^2 B^2}{\gamma^2 m_\mathrm{e}^2 c^2} \tag{10.9}$$

$$= 2\beta^2\gamma^2 c \cdot \sigma_\mathrm{T} \cdot U_\mathrm{B} \cdot \sin^2\alpha \tag{10.10}$$

where $U_\mathrm{B} = B^2/8\pi$ (Energy density of the B-fi eld), $\sigma_\mathrm{T} = \frac{8\pi e^4}{3m_\mathrm{e}^2 c^4}$ (Thomson-cross section).

Presence of σ_T due to quantum electrodynamics: Derivation of synchrotron-radiation in frame of reference of electron via interaction of electron with a virtual photon of the magnetic fi eld (i.e., Compton scattering with virtual photon).

Radiated Energy, II

Total energy radiated: Integration over all electrons.

Assumption: Isotropic velocity distribution.

Average pitch angle

$$\left\langle \sin^2\alpha \right\rangle = \frac{1}{4\pi}\int_0^{4\pi} \sin^2\alpha \, d\Omega = \frac{1}{4\pi}\int_0^{2\pi} d\varphi \int_0^{\pi} \sin^2\alpha \sin\alpha \, d\alpha = \frac{2}{3} \tag{10.11}$$

therefore

$$\langle P_{\mathrm{em}} \rangle = \frac{4}{3}\beta^2\gamma^2 c\sigma_{\mathrm{T}} U_{\mathrm{B}} \tag{10.12}$$

for $\beta \longrightarrow 1$.

Note: Since $E = \gamma m_{\mathrm{e}} c^2 \Longrightarrow P \propto E^2 U_{\mathrm{B}}$.

Note: $P_{\mathrm{em}} \propto \sigma_{\mathrm{T}} \propto m_{\mathrm{e}}^{-2} \Longrightarrow$ Synchrotron radiation from charged particles with larger mass (protons,...) is negligible.

Note: Life-time of particle of energy E is

$$t_{1/2} \sim \frac{E}{P} \propto 1/(B^2 E) = 5\,\mathrm{s}\left(\frac{B}{1\,\mathrm{T}}\right)^{-2}\gamma^{-1} = 1.6\times 10^7\,\mathrm{years}\left(\frac{B}{10^{-7}\,\mathrm{T}}\right)^{-2}\gamma^{-1} \tag{10.13}$$

Single Electron spectrum, I

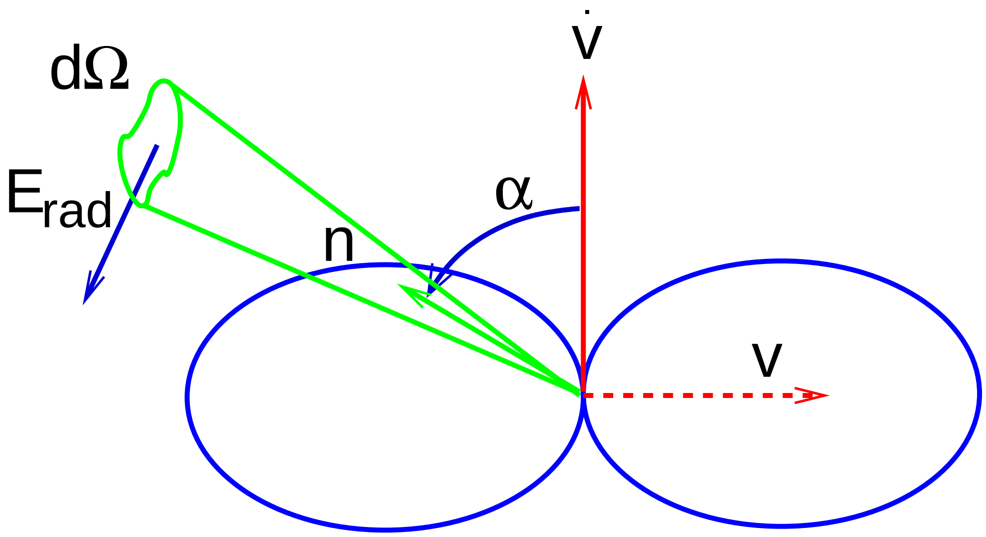

after Rybicki & Lightman, Fig. 3.5

Frame of reference of electron: Emitted radiation has dipole characteristic (see, e.g., Eq. 6.2).

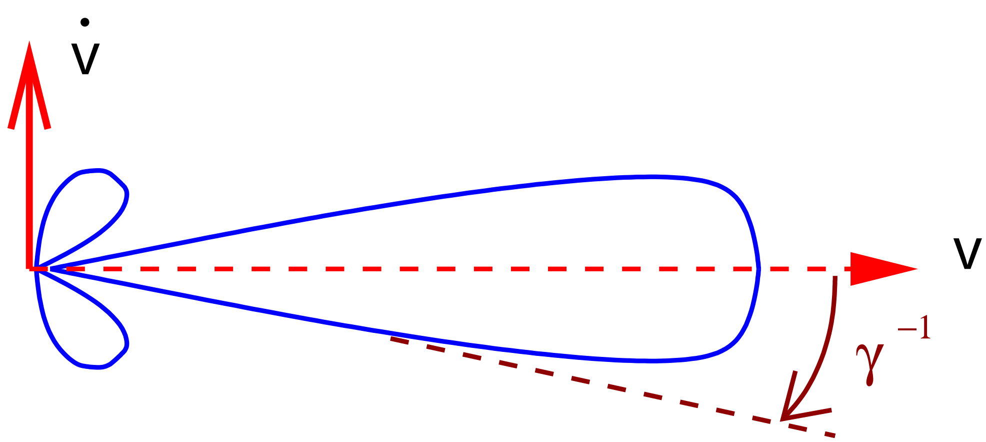

after Rybicki & Lightman, Fig. 4.11d

Lorentz-Transform into laboratory system: Forward Beaming. Opening angle is $\Delta\theta \approx \gamma^{-1}$.

Single Electron spectrum, II

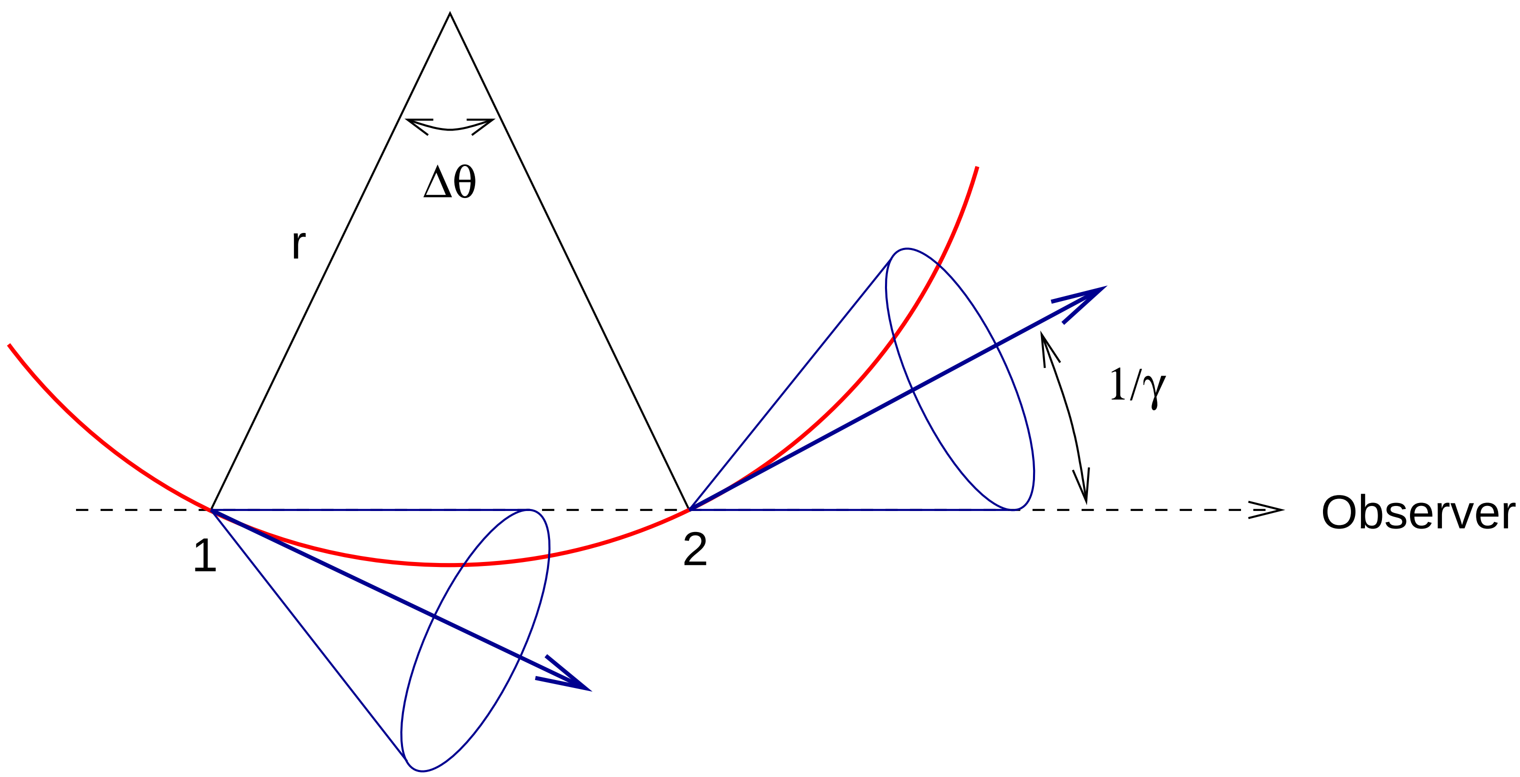

(Rybicki & Lightman, 1979, after Fig. 6.2)

Electron frame of rest: beam passes observer during time

$$\Delta t = \frac{\Delta\theta}{\omega_{\mathrm{B}}} = \frac{m_{\mathrm{e}} c\gamma}{eB}\frac{2}{\gamma} = \frac{2}{\omega_{\mathrm{L}}} \qquad (10.14)$$

Single Electron spectrum, III

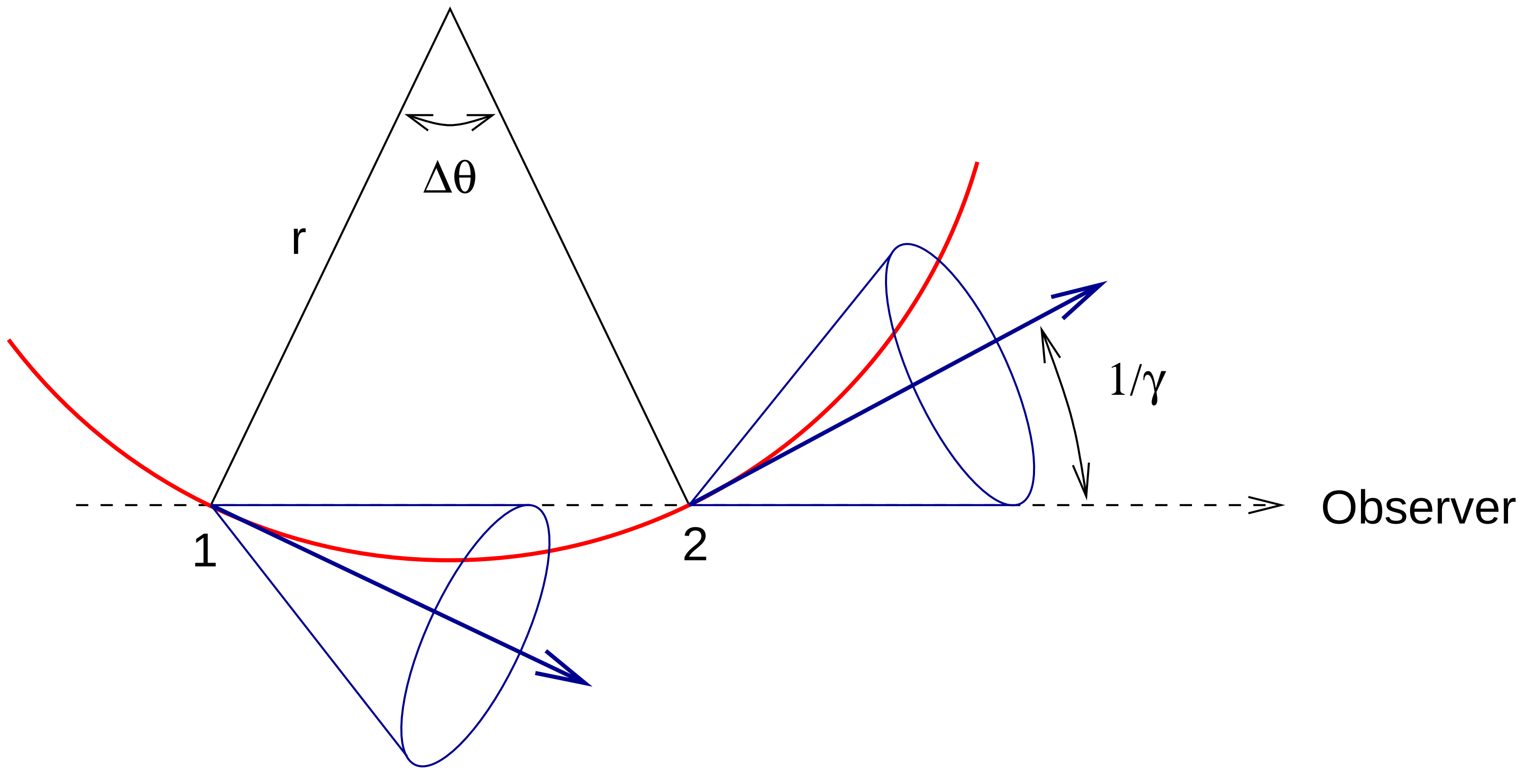

(Rybicki & Lightman, 1979, after Fig. 6.2)

Observer frame: Doppler! (electron is closer at end of beam)

$\Longrightarrow$ observed pulse duration:

$$\tau = \left(1 - \frac{v}{c}\right) \Delta t = (1 - \beta)\Delta t \tag{10.15}$$

Single Electron spectrum, IV

For $\gamma \gg 1$, i.e., $\beta = v/c \sim 1$

$$\frac{1}{\gamma^2} = 1 - \frac{v^2}{c^2} = (1+\beta)(1-\beta) \approx 2(1-\beta) \tag{10.16}$$

such that

$$\tau = (1-\beta)\Delta t = \frac{1}{2}\left(1 - \frac{v^2}{c^2}\right)\Delta t = \frac{1}{\gamma^2 \omega_{\mathrm{L}}} \tag{10.17}$$

Thus the characteristic frequency of the radiation is given by

$$\boxed{\omega_{\mathrm{c}} = \gamma^2 \omega_{\mathrm{L}} = \frac{eB}{m_{\mathrm{e}}c}\left(\frac{E}{m_{\mathrm{e}}c^2}\right)^2} \tag{10.18}$$

Resulting Field

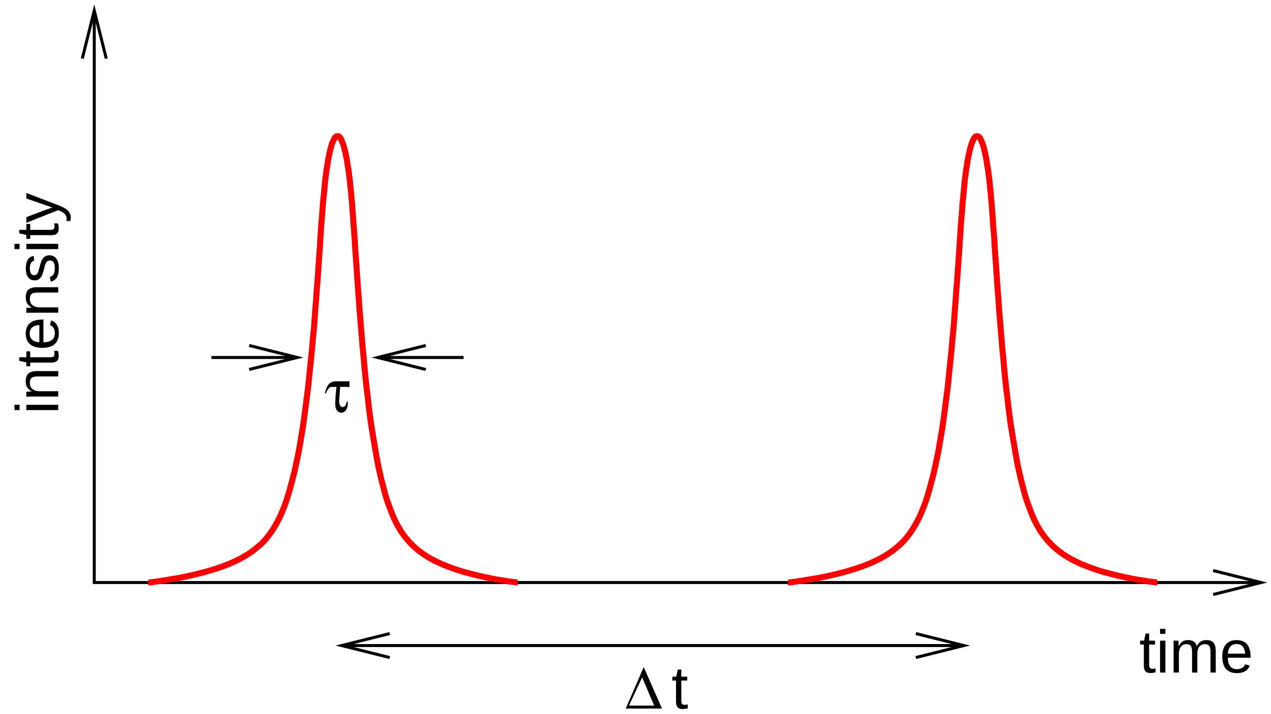

after Shu, Fig. 18.2

The observed time-dependent E-Field, $E(t)$, from one electron is a sequence of pulses of width τ, separated in time by Δt.

To a good precision, we can approximate these single peaks with δ-functions.

In reality: derive spectrum by Fourier-transforming $E(t)$. Basic result is the same.

Nonthermal Synchrotron Radiation, I

Spectral energy distribution P_ν of one electron with total energy $E = \gamma m_\mathrm{e} c^2$ is

$$P_\nu(\gamma) = \frac{4}{3}\beta^2\gamma^2 c\sigma_\mathrm{T} U_\mathrm{B} \delta(\nu - \gamma^2\nu_\mathrm{L}) \tag{10.19}$$

where $\delta(x)$ is a δ-function, i.e.,

$$\delta(x) = 0 \quad \text{for } x \neq 0 \quad \text{and} \quad \int_{-\infty}^{+\infty} \delta(x)\, dx = 1 \tag{10.20}$$

i.e., electron with energy $\gamma m c^2$ “blinks” at frequency $\nu = \gamma^2\nu_\mathrm{L} = 1/\tau$.

For an electron distribution, $n(\gamma)$, the emitted spectrum is found by properly weighting contributions of electrons with different energies:

$$P_\nu = \int_1^\infty P_\nu(\gamma) n(\gamma) d\gamma \tag{10.21}$$

Most important case: nonthermal synchrotron radiation, where electrons have a power-law distribution

$$n(\gamma) d\gamma = n_0 \gamma^{-p} d\gamma \tag{10.22}$$

Nonthermal Synchrotron Radiation, II

Insert distribution into Eq. (10.21) and perform the integration:

$$P_\nu = \int_1^\infty \frac{4}{3}\beta^2\gamma^2 c\sigma_\mathrm{T} U_\mathrm{B}\delta(\nu - \gamma^2\nu_\mathrm{L}) n_0 \gamma^{-p} d\gamma \tag{10.23}$$

since $\gamma \gg 1$: $\beta \approx 1$

$$= A\int_1^\infty \gamma^{2-p}\delta(\nu - \gamma^2\nu_\mathrm{L}) d\gamma \tag{10.24}$$

substituting $\nu' = \gamma^2\nu_\mathrm{L}$, i.e., $d\nu' = \nu_\mathrm{L} 2\gamma d\gamma$

$$= B\int_{\nu_\mathrm{L}}^\infty \gamma^{1-p}\delta(\nu - \nu') d\nu' \tag{10.25}$$

since $\gamma = (\nu'/\nu_\mathrm{L})^{1/2}$, one finally finds

$$P_\nu = \frac{2}{3} c\sigma_\mathrm{T} n_0 \frac{U_B}{\nu_\mathrm{L}} \left(\frac{\nu}{\nu_\mathrm{L}}\right)^{-\frac{p-1}{2}} \tag{10.26}$$

The spectrum of an electron power-law distribution is a power-law!

Nonthermal Synchrotron Radiation, III

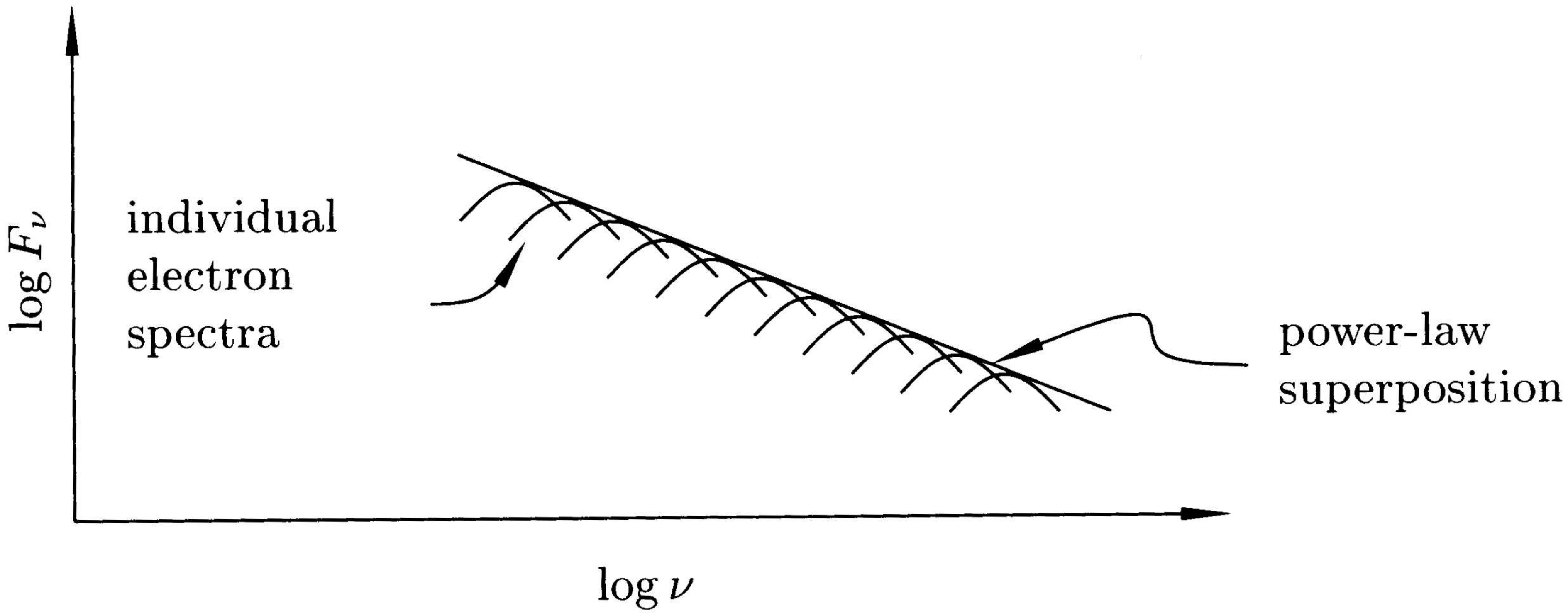

Shu, Fig. 18.4

Summary

What we have done so far:

1. Motion of the electron
2. Radiation characteristic from relativistic motion
3. Doppler-effect
4. Integration over electron distribution

It is possible to do the same analytically without any approximations. This is too complicated to be done here. See the references for details.

Exact Results, I

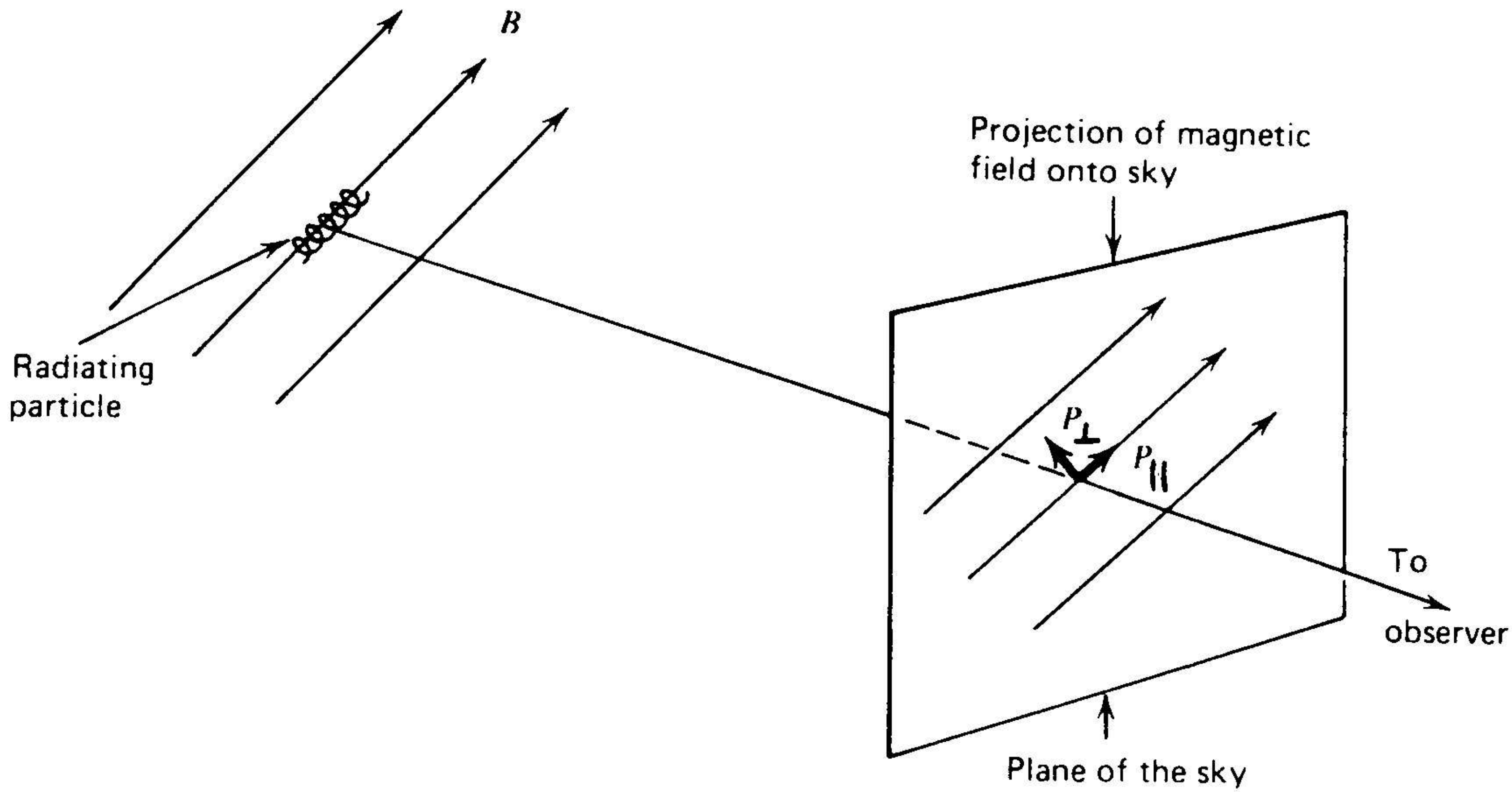

(Rybicki & Lightman, 1979, Fig. 6.7)

Exact calculation needs to take into account polarization of synchrotron radiation.

Exact Results, II

Result of exact calculation for both polarization directions:

$$\begin{pmatrix} P_{\parallel} \\ P_{\perp} \end{pmatrix} = \frac{\sqrt{3}}{2}\frac{e^3 B}{mc^2} \begin{pmatrix} F(\nu/\nu_{\mathrm{c}}) - G(\nu/\nu_{\mathrm{c}}) \\ F(\nu/\nu_{\mathrm{c}}) + G(\nu/\nu_{\mathrm{c}}) \end{pmatrix} \tag{10.27}$$

where

$$F(x) = x \int_x^\infty K_{5/3}(y)\,dy \tag{10.28}$$

$$G(x) = x K_{2/3}(x) \tag{10.29}$$

and K_i are modified Bessel-functions of i-th order

Polarization allows to measure the magnetic field direction

$$F(x) = x\int_x^\infty K_{5/3}(\eta)\,d\eta \quad \text{and} \quad G(x) = xK_{2/3}(x)$$

x	$F(x)$	$G(x)$	x	$F(x)$	$G(x)$
0	0	0	0.90	0.694	0.521
0.001	0.213	0.107	1.0	0.655	0.494
0.005	0.358	0.184	1.2	0.566	0.439
0.01	0.445	0.231	1.4	0.486	0.386
0.025	0.583	0.312	1.6	0.414	0.336
0.050	0.702	0.388	1.8	0.354	0.290
0.075	0.772	0.438	2.0	0.301	0.250
0.10	0.818	0.475	2.5	0.200	0.168
0.15	0.874	0.527	3.0	0.130	0.111
0.20	0.904	0.560	3.5	0.0845	0.0726
0.25	0.917	0.582	4.0	0.0541	0.0470
0.29	0.918	0.592	4.5	0.0339	0.0298
0.30	0.918	0.596	5.0	0.0214	0.0192
0.40	0.901	0.607	6.0	0.0085	0.0077
0.50	0.872	0.603	7.0	0.0033	0.0031
0.60	0.832	0.590	8.0	0.0013	0.0012
0.70	0.788	0.570	9.0	0.00050	0.00047
0.80	0.742	0.547	10.0	0.00019	0.00018

Total Emitted Spectrum

The total emitted power for monoenergetic electrons is

$$P(\nu) = P_{\|}(\nu) + P_{\perp}(\nu) \propto F(\nu) \tag{10.30}$$

As before, the total emitted spectrum is found by integrating over the electron energy distribution. For a power-law:

$$\begin{pmatrix} P_{\|}(\nu) \\ P_{\perp}(\nu) \end{pmatrix} = \left(\frac{\sqrt{3}}{2}\right) n_0 \frac{e^3 B}{m_\mathrm{e} c^2} \begin{pmatrix} J_F - J_G \\ J_F + J_G \end{pmatrix} \left(\frac{2\nu}{3\nu_\mathrm{L}}\right)^{-(p-1)/2} \tag{10.31}$$

where

$$J_F = \frac{2^{(p+1)/2}}{p+1} \Gamma\left(\frac{p}{4} + \frac{19}{12}\right) \Gamma\left(\frac{p}{4} - \frac{19}{12}\right) \tag{10.32}$$

$$J_G = 2^{(p-3)/2} \Gamma\left(\frac{p}{4} + \frac{7}{12}\right) \Gamma\left(\frac{p}{4} - \frac{1}{12}\right) \tag{10.33}$$

$\Gamma(x) = \int_0^\infty t^{-x} e^{-t} dt$ is the Gamma-function.

Degree of Polarization

The degree of polarization is defined by

$$\boxed{\text{degree of polarization} := \frac{P_\perp - P_\parallel}{P_\perp + P_\parallel}} \quad (10.34)$$

For a power law electron distribution:

$$\boxed{\frac{P_\perp - P_\parallel}{P_\perp + P_\parallel} = \frac{J_G}{J_F} = \frac{p+1}{p+7/3}} \quad (10.35)$$

For $p = 2.5$ the degree of polarization is $\sim 70\%$. This is very large!!

Caveat: Faraday-rotation and B-fi eld inhomogeneities can decrease the degree of polarization.

Synchrotron Self-Absorption

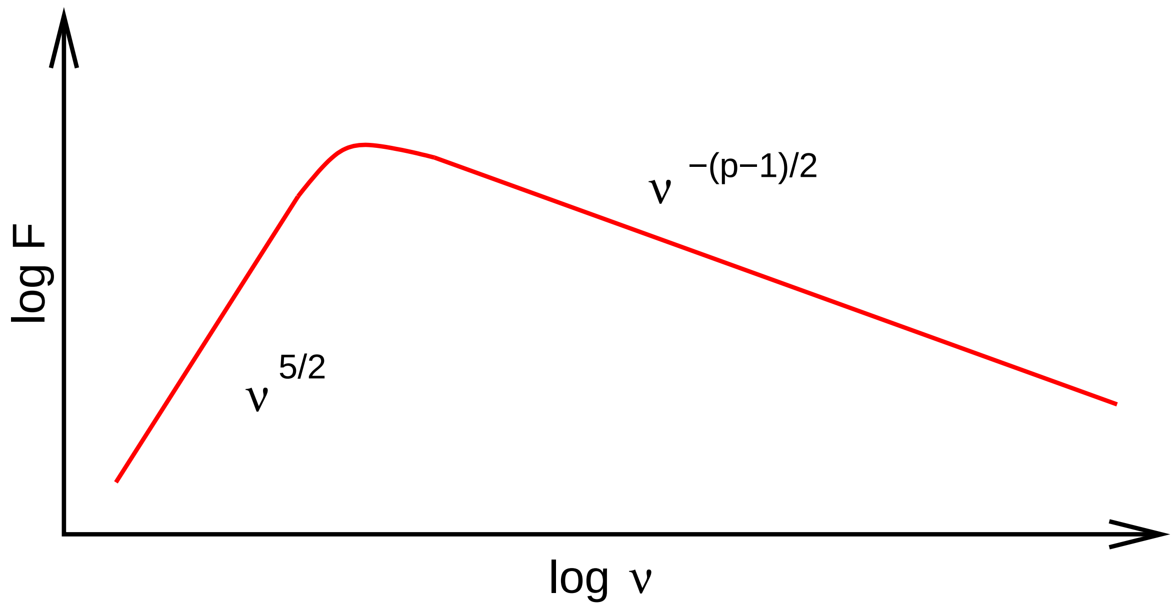

after Shu, Fig. 18.6

At low ν: synchrotron emitting electrons can absorb synchrotron photons: synchrotron self-absorption.

For a power law electron distribution $\propto E^{-p}$, total spectral shape is:

For low frequencies: $P_\nu \propto B^{-1/2}\nu^{5/2}$ (independent of p!)

For large frequencies: $P_\nu \propto \nu^{-(p-1)/2}$

At very high frequencies, additional break due to electron energy losses. The transition frequency can be used to measure the strength of the B-Field. See text-books on radio astronomy.

The M87 Jet

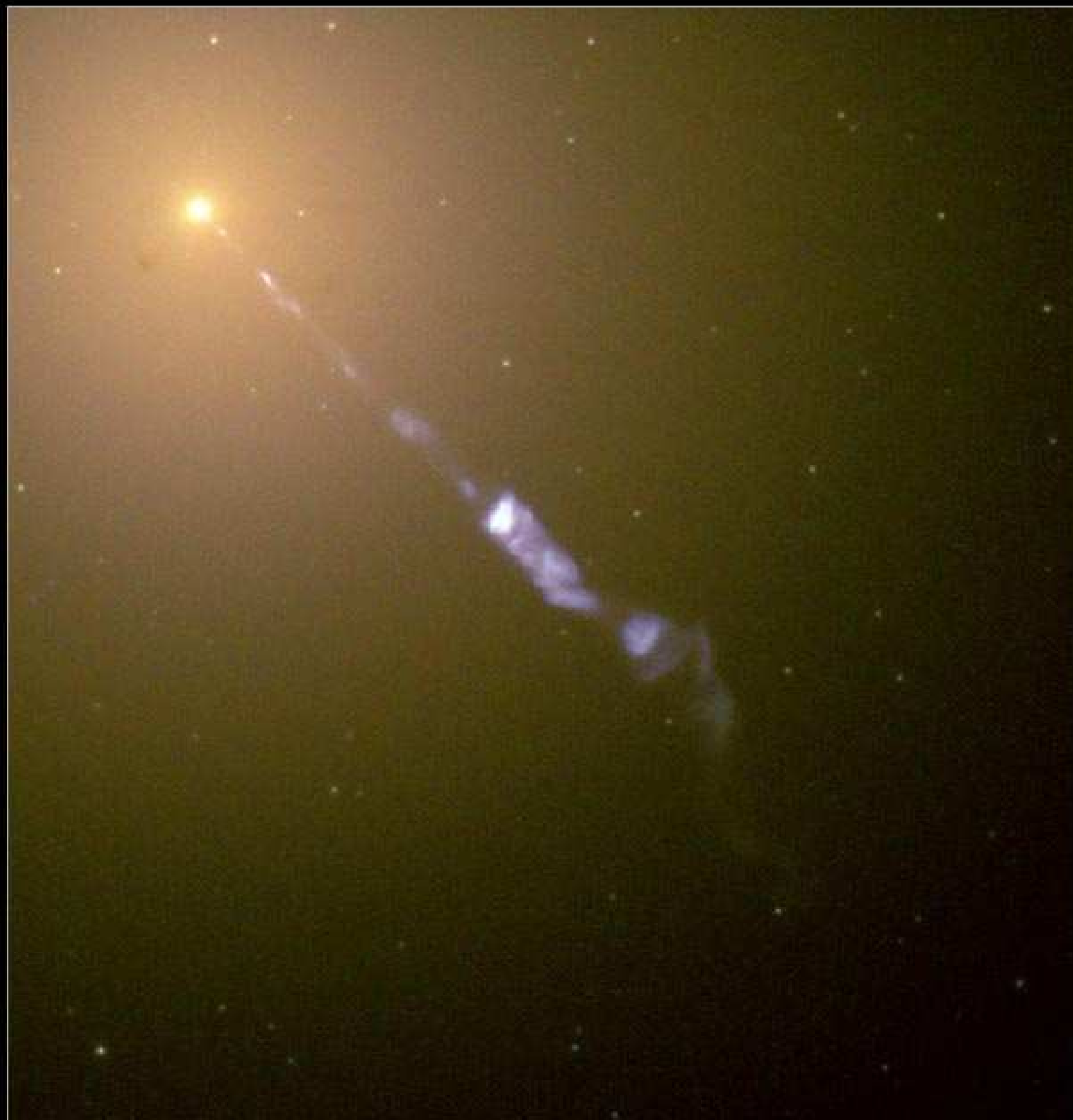

Hubble Heritage

PRC00-20 • Space Telescope Science Institute • NASA and The Hubble Heritage Team (STScI/AURA)

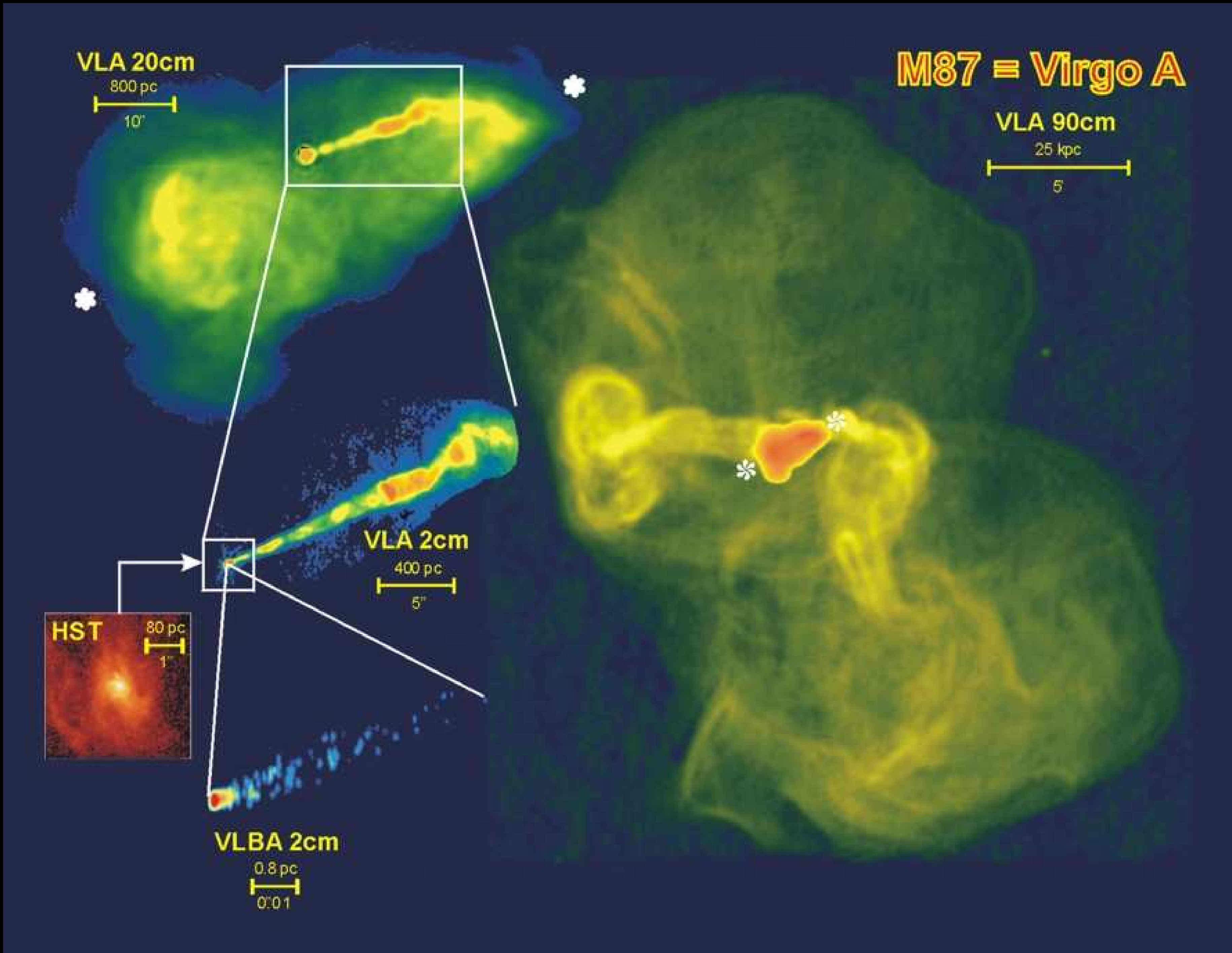

VLA 20cm
800 pc
10"
M87 ≡ Virgo A
VLA 90cm
25 kpc
5'
VLA 2cm
400 pc
5"
HST
80 pc
1"
VLBA 2cm
0.8 pc
0.01

NRAO/AUI

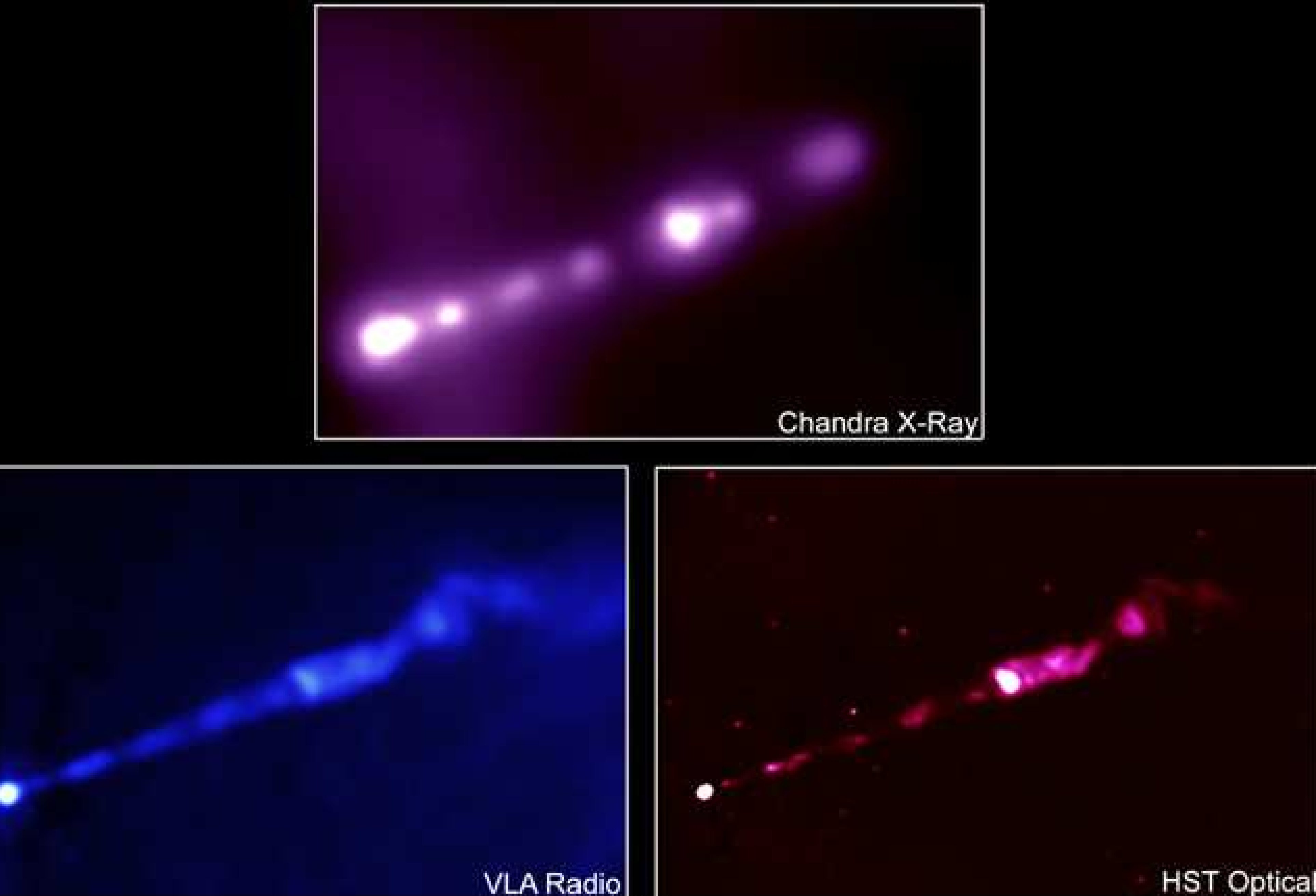
Chandra X-Ray
VLA Radio
HST Optical

Jet Spectrum

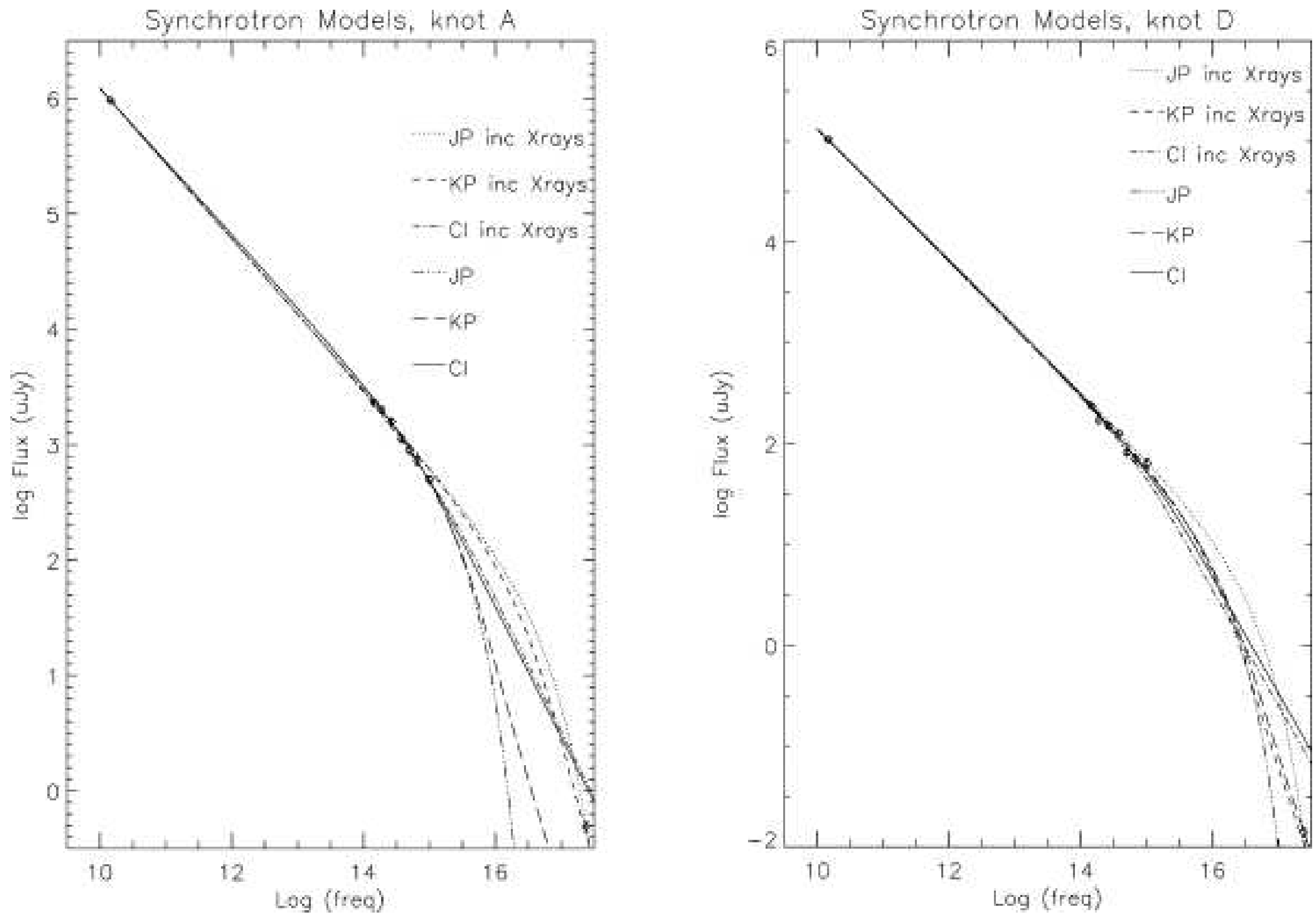

(M87; Perlman et al., 2002)

Spectral shape of jet emission is a power law $\Longrightarrow$ synchrotron radiation

Typical power law index: $\alpha \sim 0.65$ between radio and optical.

Jet Polarization

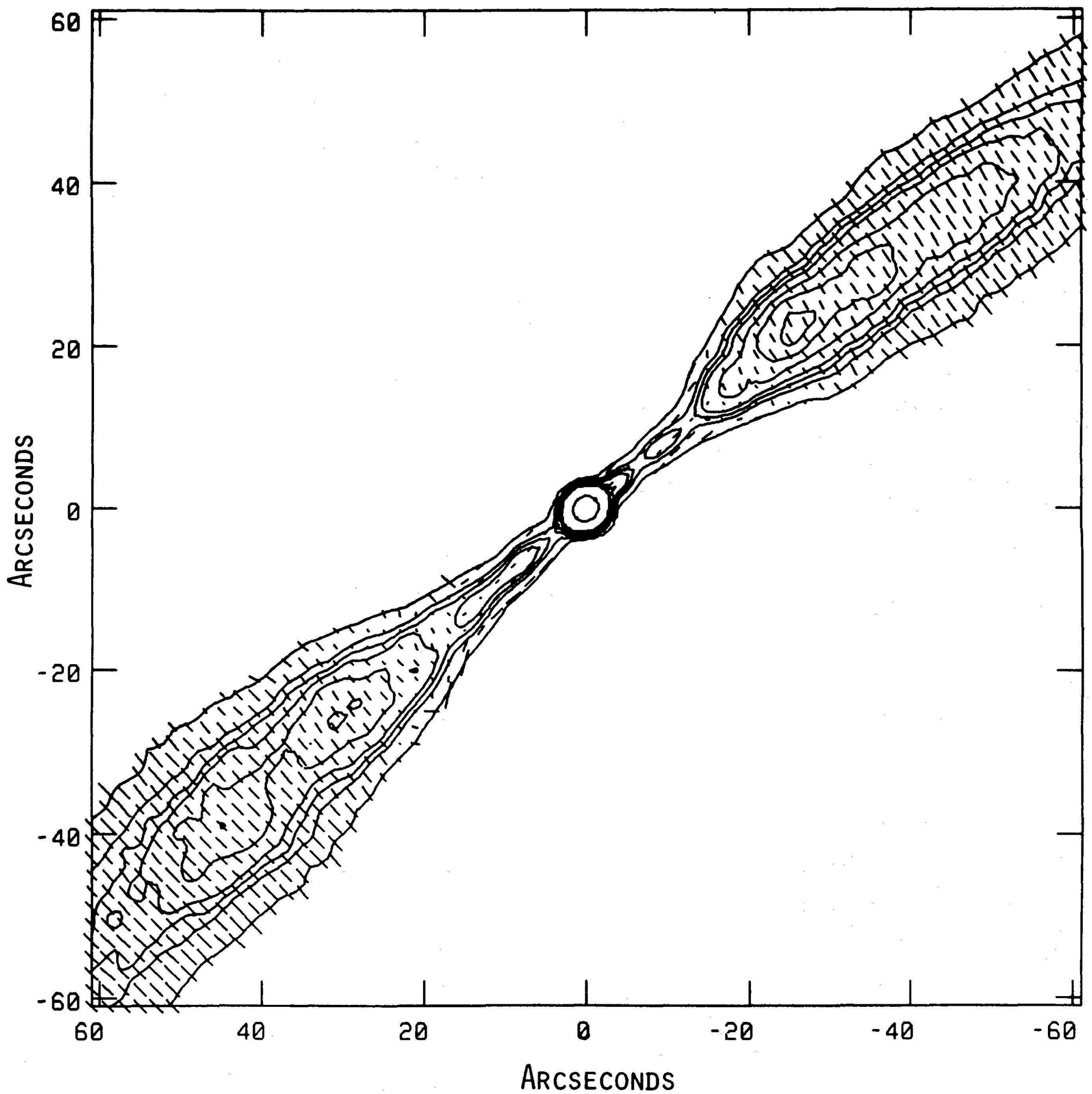

polarization in two-sided jet sources (FR 1): up to 40%

B-field orientation:

- close to core: $B \parallel$ jet axis
- away from core (~10% jet length): $B \perp$ jet axis

B-fi eld can change orientation again in knots

(B-fi eld confi guration in IC 4296; Killeen, Bicknell & Ekers, 1986, Fig. 25b)

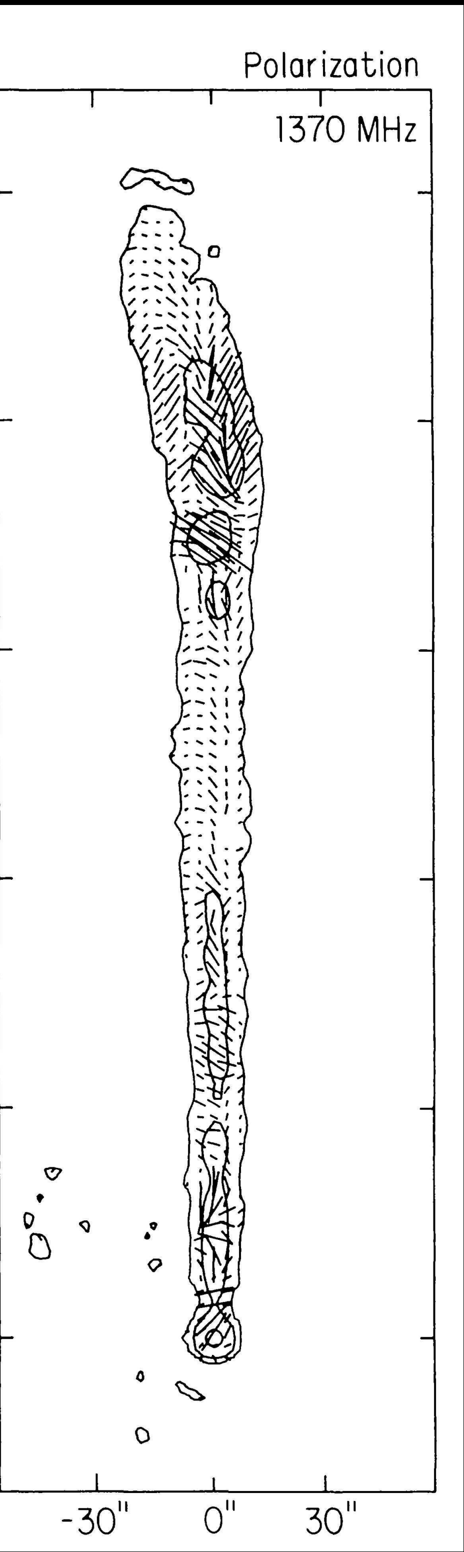

polarization in one-sided jet sources (FR 2): similar to FR 1, i.e., 40% and higher

B-field orientation in FR 2: parallel to jet axis throughout the jet

(E-fi eld confi guration in NGC 6251, note: B-fi eld is perpendicular to E-fi eld!;Perley, Bridle & Willis, 1984, Fig. 17)

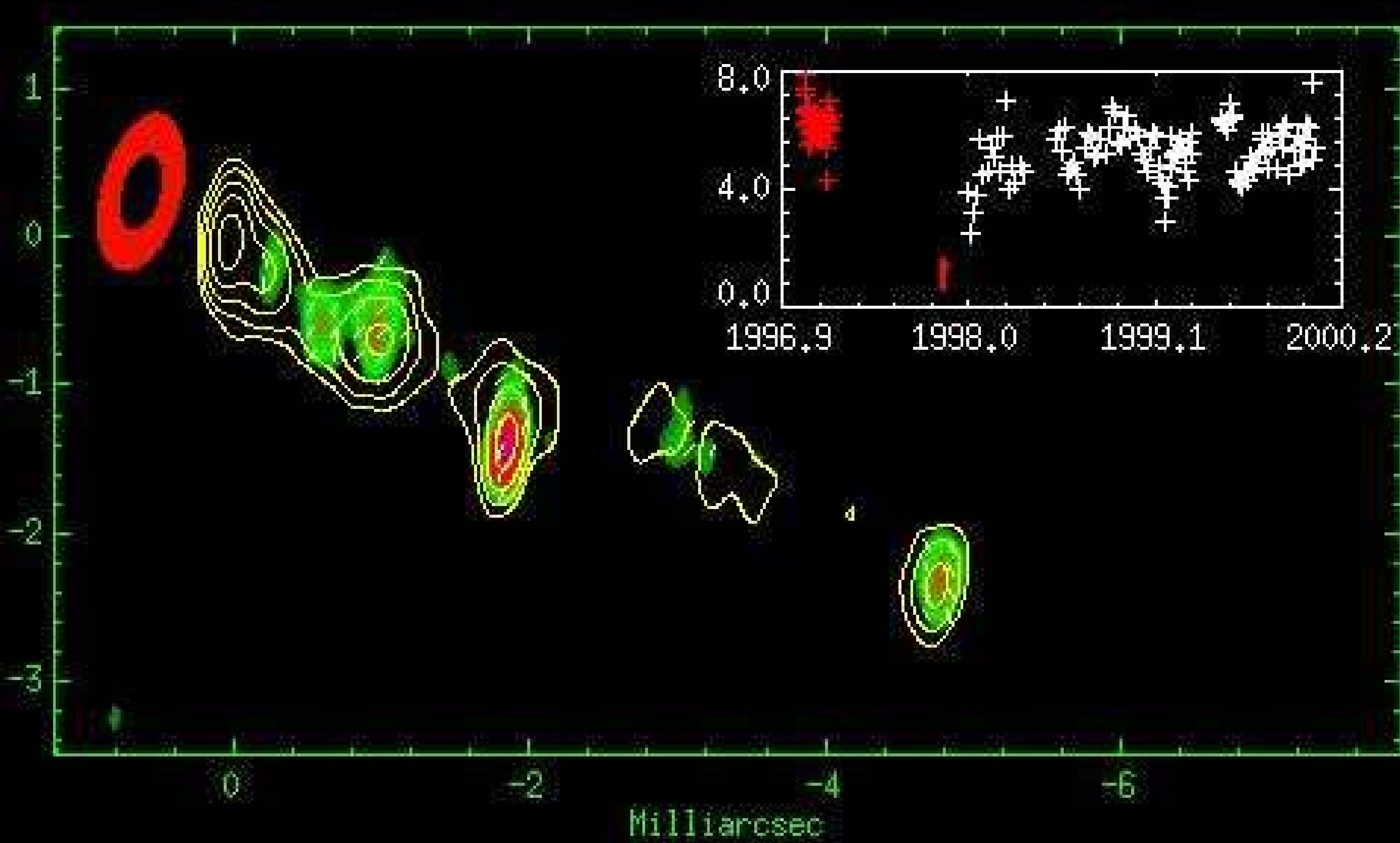

Jet motion in 3C120 (Marscher et al., 2002)

3C120: Sy 1, $M_{\rm BH} = 3 \times 10^7\,M_\odot$ from reverberation mapping

MOVIE TIME: `jetmovies/3c120rx.avi`

Superluminal Motion, II

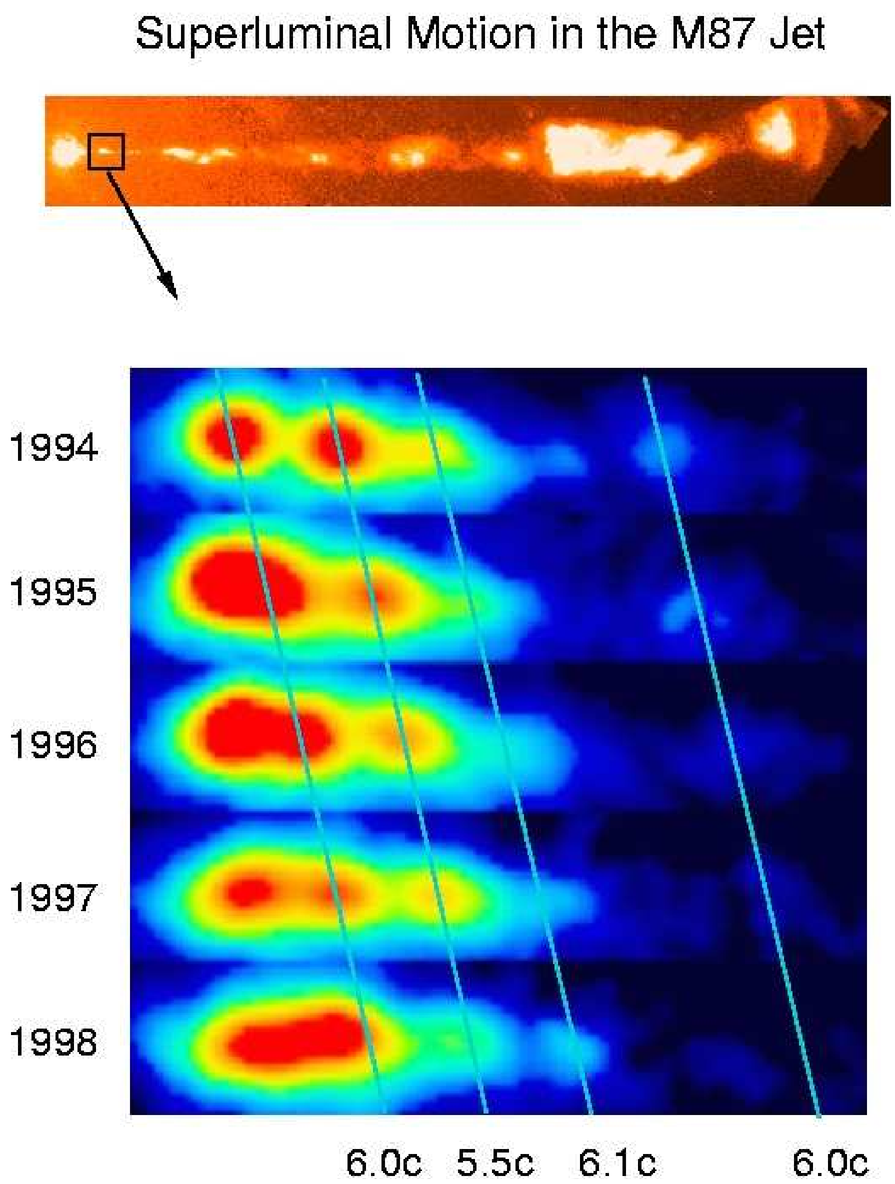

3C120: Apparent speed of jet: $\sim 5c$

M87: Apparent speed of jet: $\sim 6c$

Superluminal motion: The apparent velocities measured in many AGN jets are $v > c$.

First discovered in 1971 in 3C273.

Biretta/STScI

Superluminal Motion, III

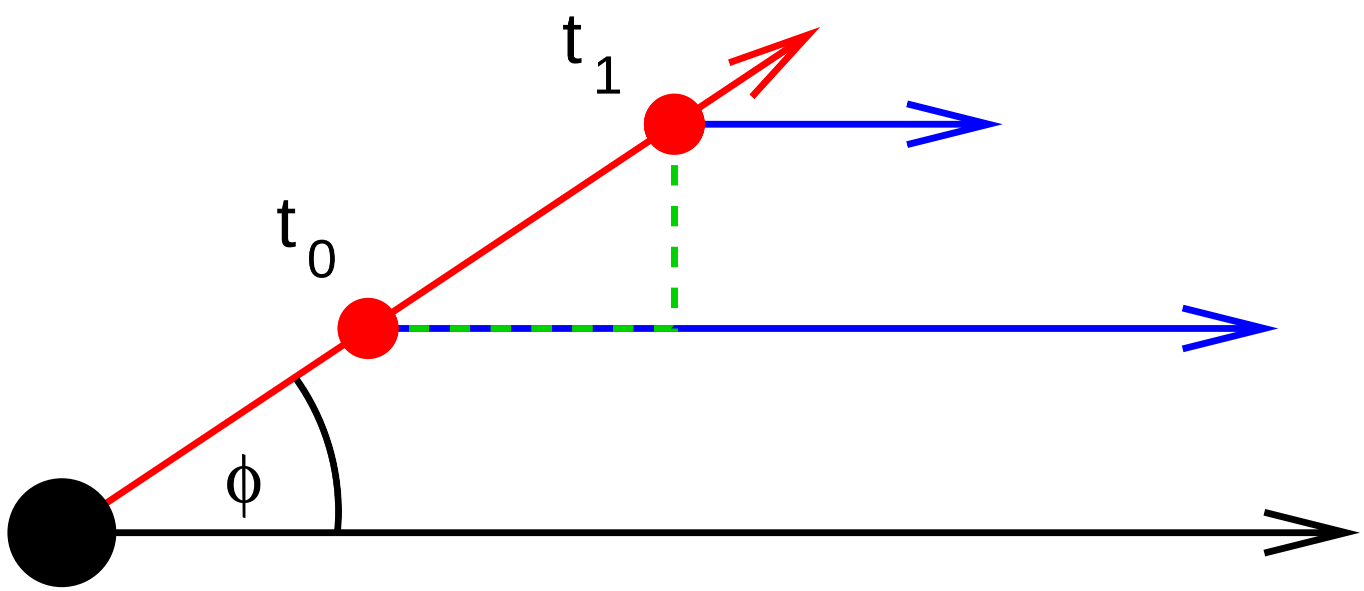

Consider blob moving towards us with speed v and angle ϕ with respect to line of sight, emitting light signals at t_0 and $t_1 = t_0 + \Delta t_\mathrm{e}$

Light travel time: Observer sees signals separated by

$$\Delta t_\mathrm{o} = \Delta t_\mathrm{e} - \Delta t_\mathrm{e} \frac{v}{c} \cos\phi = \left(1 - \frac{v}{c}\cos\phi\right) \Delta t_\mathrm{e} \qquad (10.36)$$

Observed distance traveled in plane of sky:

$$\Delta \ell_\perp = v \Delta t_\mathrm{e} \sin\phi \qquad (10.37)$$

Superluminal Motion, IV

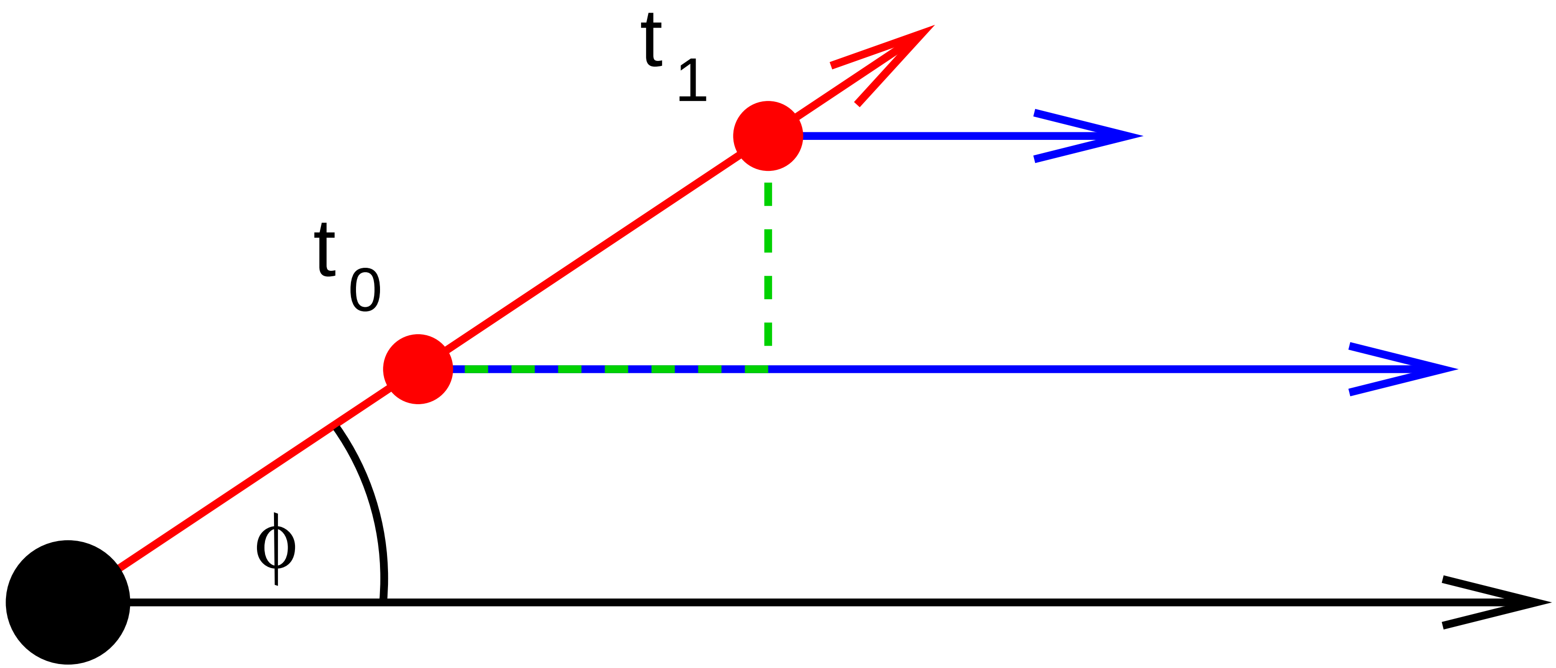

Apparent velocity deduced from observations:

$$v_{\mathrm{app}} = \frac{\Delta \ell_\perp}{\Delta t_{\mathrm{o}}} = \frac{v \Delta t_{\mathrm{e}} \sin\phi}{\left(1 - \frac{v}{c}\cos\phi\right)\Delta t_{\mathrm{e}}} = \frac{v \sin\phi}{\left(1 - \frac{v}{c}\cos\phi\right)} \tag{10.38}$$

$\Longrightarrow$ For v/c large and ϕ small: $v_{\mathrm{app}} > c$

Superluminal Motion, V

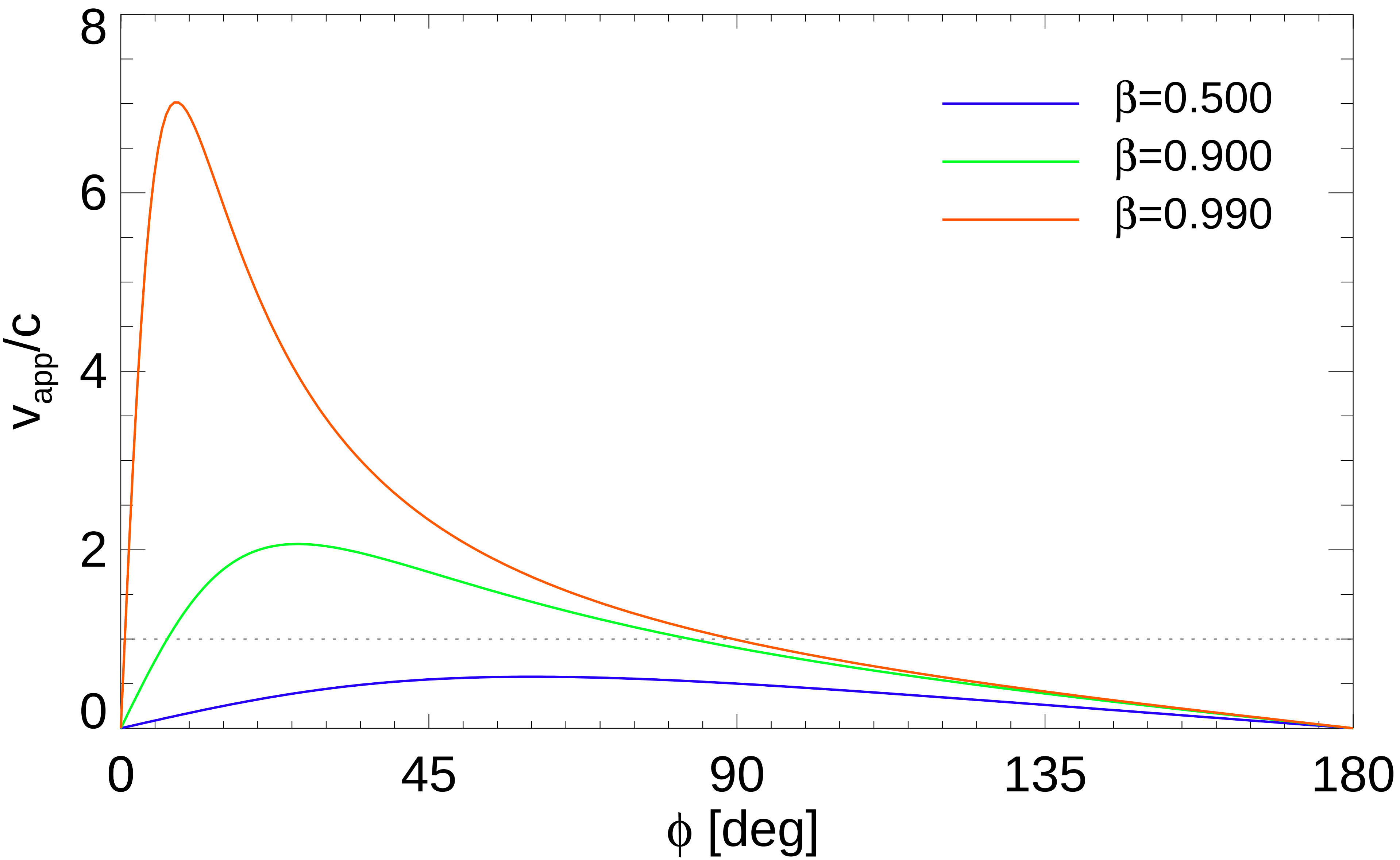

A relativistic invariant, I

So, if ϕ is known, we can determine real speed.

In order to determine ϕ, we have to make use of an useful relativistic invariant:

$$\frac{I_{\mathrm{nu}}}{\nu^3} = \text{const.} \tag{10.39}$$

in all frames of reference.

Proof: The number of photons with momentum in interval $\mathbf{p}, \mathbf{p} + d^3$ is given by

$$dN = 2n \left(\frac{V\, d^3 p}{h^3} \right) \tag{10.40}$$

where n: photon number, $V\, d^3p$: phase volume, h^3: volume of phase space cell.

$\Longrightarrow$ Energy flowing through volume element $d^3x = \; dA(c\,dt)$:

$$dE = h\nu\, dN = 2nh\nu\, dA(c\,dt) \left(\frac{d^3p}{h^3} \right) \tag{10.41}$$

A relativistic invariant, II

Since $p = h\nu/c$:

$$d^3p = p^2\,dp\,d\Omega = \left(\frac{h\nu}{c}\right)^2 h\frac{d\nu}{c}\,d\Omega = \left(\frac{h}{c}\right)^3 \nu^2\,d\nu\,d\Omega \tag{10.42}$$

Therefore

$$dE = 2nh\nu c\,dA\,dt\left(\frac{d^3p}{h^3}\right) = \frac{2h\nu^3}{c^2}n\,dA\,dt\,d\Omega\,d\nu \tag{10.43}$$

or

$$\frac{dE}{dA\,dt\,d\Omega\,d\nu} = I = \frac{2h\nu^3}{c^2}n \tag{10.44}$$

Therefore

$$\frac{I}{\nu^3} = \frac{2h}{c^2}n \tag{10.45}$$

and since n is just a number, I/ν^3 is Lorentz-invariant.

Relativistic Aberration

Relativistic invariance: $I_\nu/\nu^3 = $ const. where I_ν is the intensity.

Therefore, observed intensity of a moving blob:

$$\frac{I(\nu_{\text{obs}})}{\nu_{\text{obs}}^3} = \frac{I(\nu_{\text{em}})}{\nu_{\text{em}}^3} \tag{10.46}$$

Because of the relativistic Doppler effect:

$$\nu_{\text{obs}} = \frac{\nu_{\text{em}}}{\gamma(1-\beta\cos\phi)} \tag{10.47}$$

($\beta = v/c$) and thus

$$I(\nu_{\text{obs}}) = \nu_{\text{obs}}^3 \frac{I(\nu_{\text{em}})}{\nu_{\text{em}}^3} = \frac{I(\nu_{\text{em}})}{(\gamma(1-\beta\cos\phi))^3} \tag{10.48}$$

Specifi cally, for a blob with a power law spectrum:

$$I(\nu_{\text{obs}}) = \frac{A\nu_{\text{em}}^{-\alpha}}{(\gamma(1-\beta\cos\phi))^3} = \frac{A\,(\gamma(1-\beta\cos\phi))^{-\alpha}\,\nu_{\text{obs}}^{-\alpha}}{(\gamma(1-\beta\cos\phi))^3} = \frac{A\nu_{\text{obs}}^{-\alpha}}{(\gamma(1-\beta\cos\phi))^{3+\alpha}} \tag{10.49}$$

(where A is the normalization constant of the power law).

Relativistic Aberration

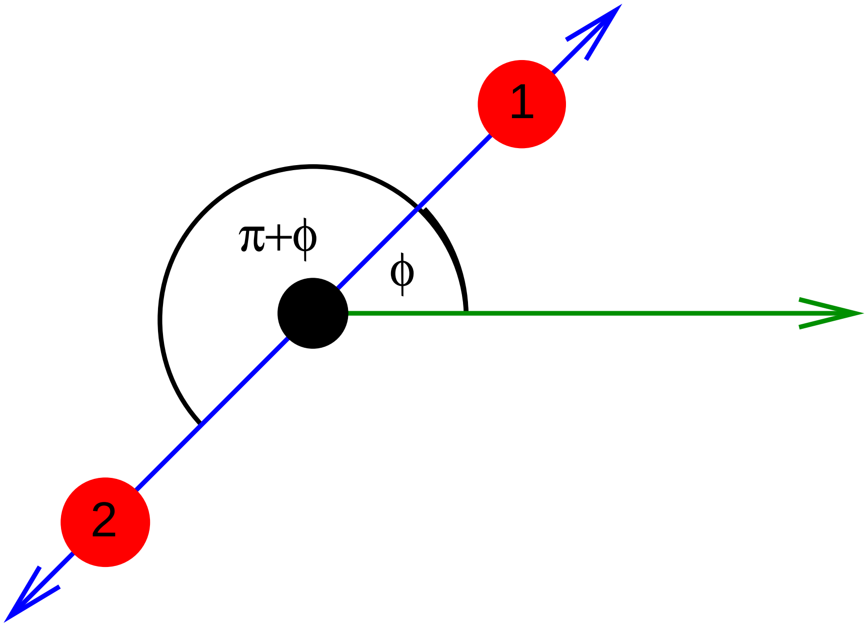

Now take a source emitting blobs symmetrically in two directions.

From Eq. (10.49) the ratio of fluxes from the blobs is

$$\frac{F_1}{F_2} = \left(\frac{1+\beta\cos\phi}{1-\beta\cos\phi}\right)^{3+\alpha} \tag{10.50}$$

Radiation from a blob moving towards observer is strongly boosted.

Jet can be expressed as a series of blobs. But the number of blobs observed scales as $(\gamma(1-v\cos\phi))^{-1}$, such that for jets:

$$\frac{F_1}{F_2} = \left(\frac{1+\beta\cos\phi}{1-\beta\cos\phi}\right)^{2+\alpha} \tag{10.51}$$

One sidedness of jets is a relativistic effect.

From measuring F_1/F_2, we can in principle determine ϕ.

Relativistic Aberration

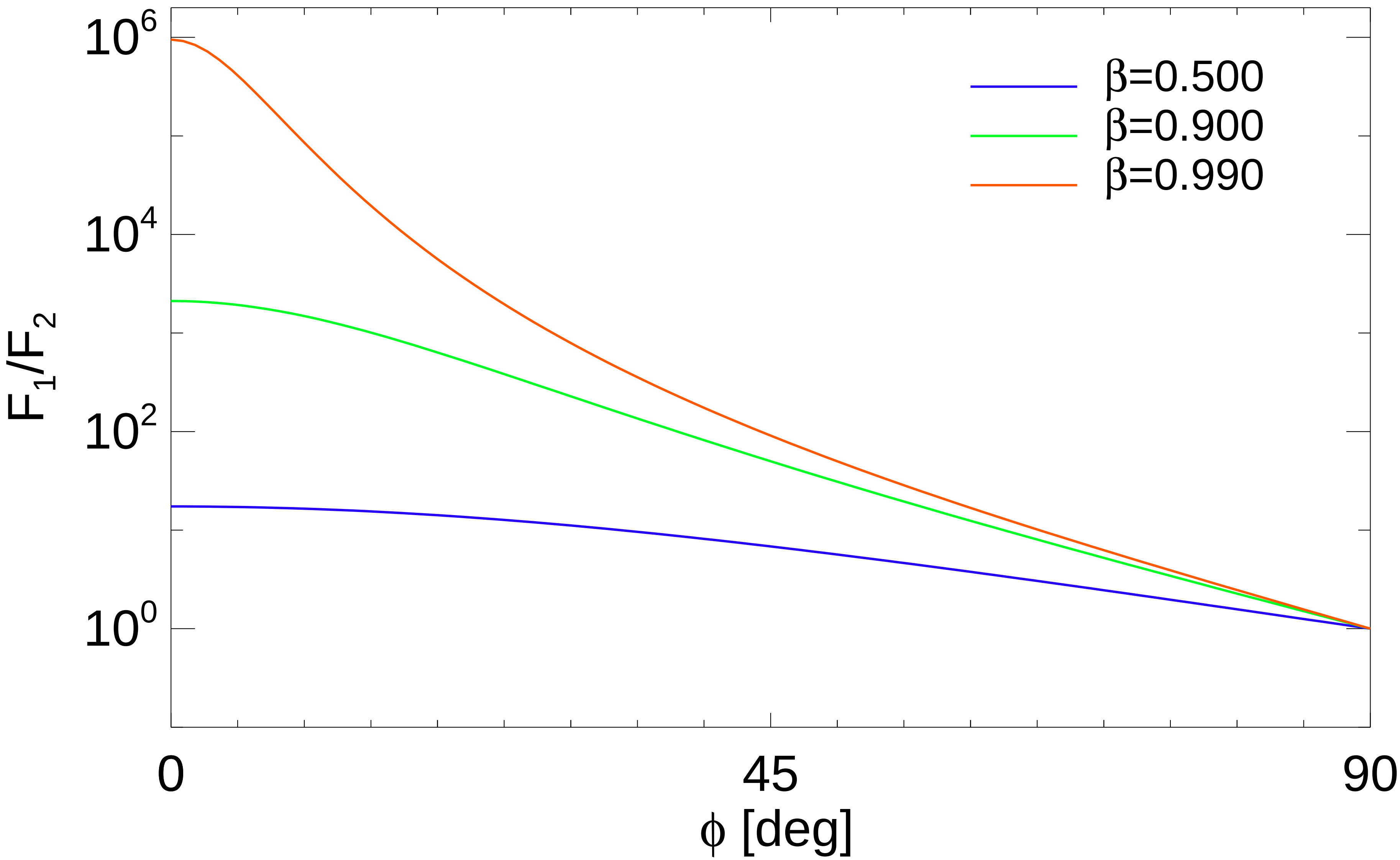

Jet Statistics, I

Kellermann et al. (2004): Largest survey of jets performed so far.

- Wavelength 2 cm (15 GHz)
- All AGN with flat spectra ($\alpha < 0.5$ for $S_\nu \propto \nu^{-\alpha}$) and fluxes above 1.5 Jy at 15 GHz
- Survey started in 1994, ended in 2001, typically 7 observations per source
- 208 features in 110 AGN (Seyfert, BL Lac, Quasars).
- movies and images at `http://www.nrao.edu/2cmsurvey` (recommended!)

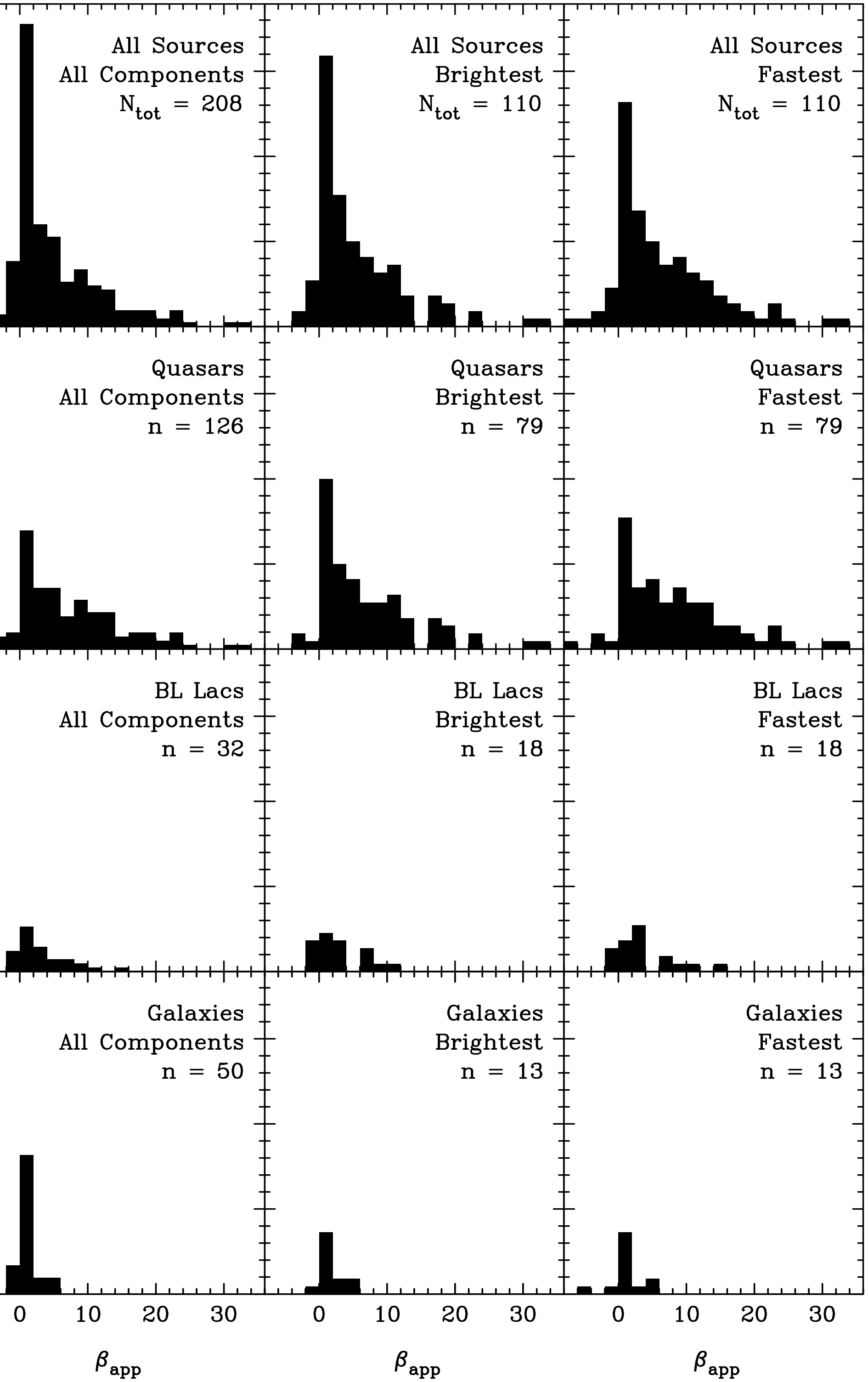

Distribution of observed velocities:

- apparent velocity range: $\beta \leq 15$
- Quasars: tail up to $\beta \sim 34$
- others: mainly $\beta \lesssim 6$

(Kellermann et al., 2004, Fig. 4)

Jet Statistics, III

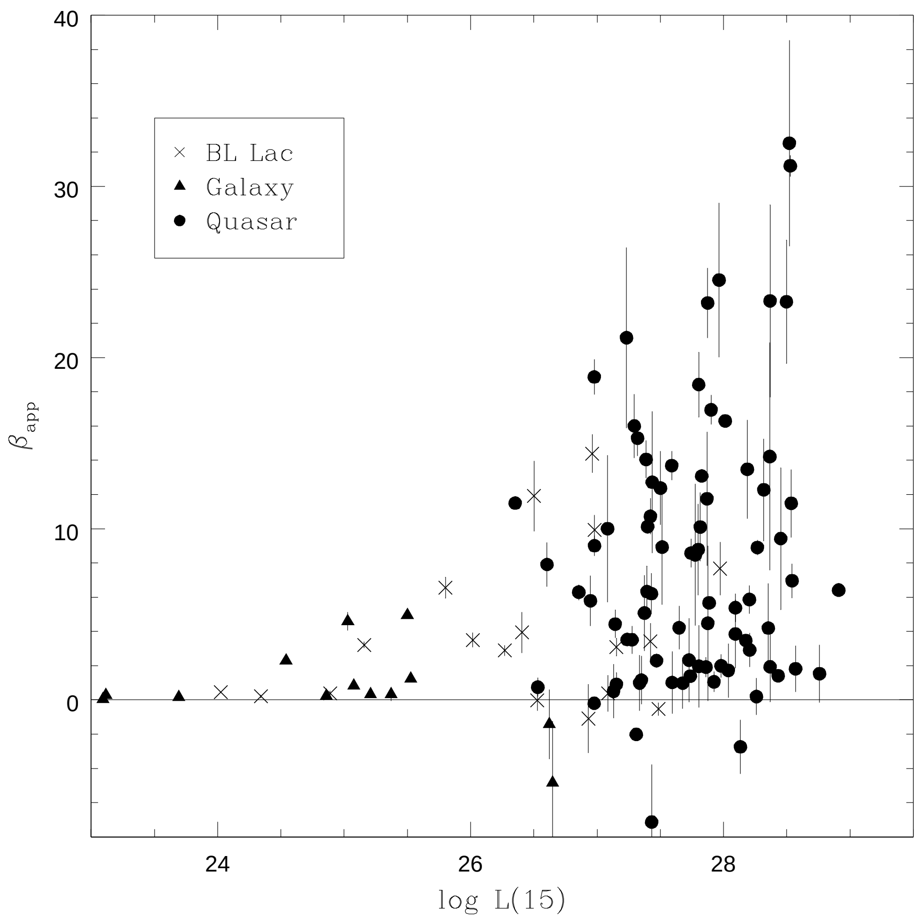

(Kellermann et al., 2004, Fig. 6)

Relation between β and luminosity:
larger scatter at higher L

This does *not* mean that lower L sources have lower speeds, since observational effects also play a role:
sample is flux limited
$\Longrightarrow$ faintest sources are close, and probably represent the most normal sources
$\Longrightarrow$ probability that high Lorentz factor jets point in our direction grows with sampled volume, so perhaps the distribution is a selection effect.

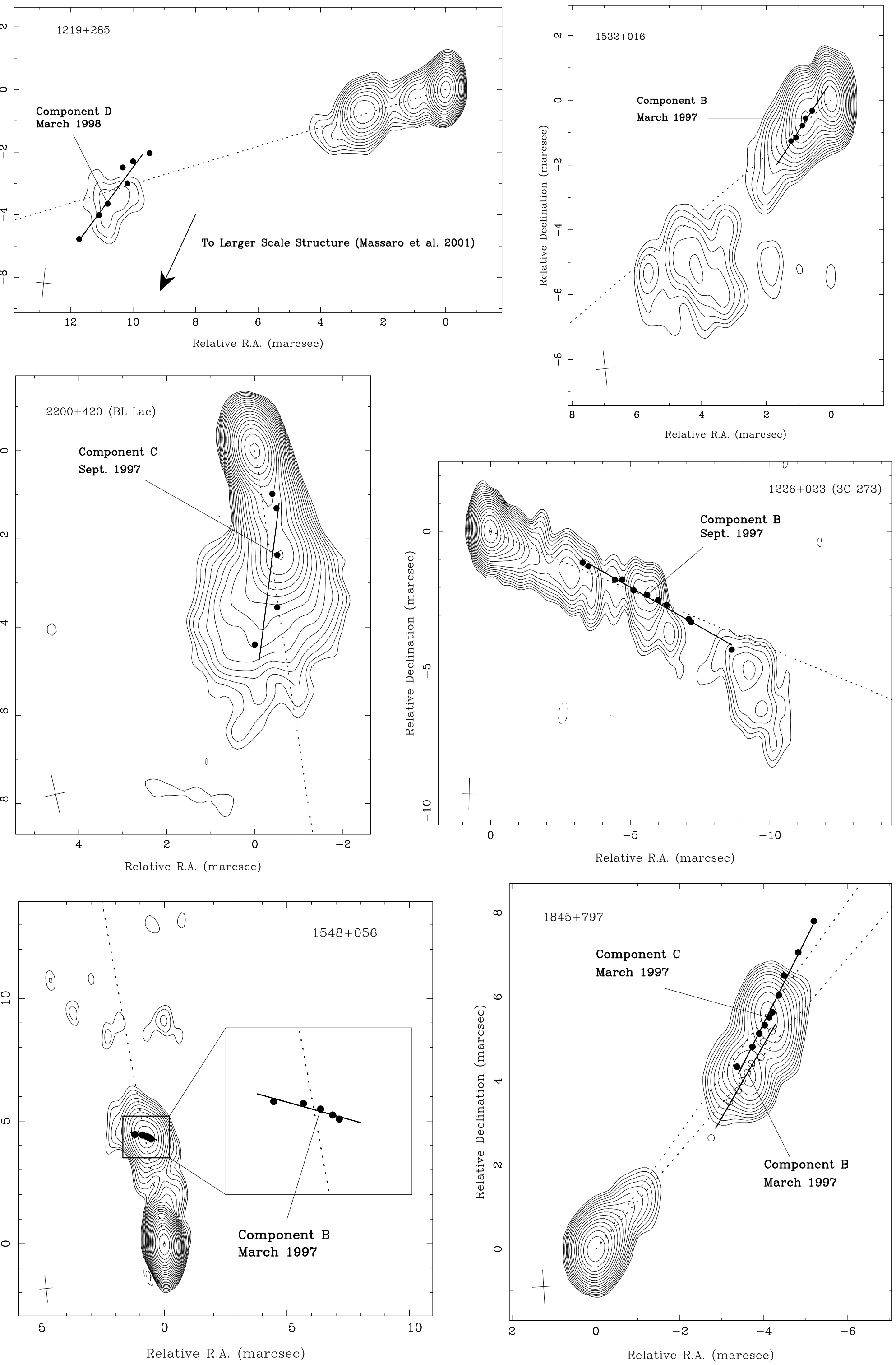

In many sources, bent trajectories are observed, which do not follow jet axis

$\Longrightarrow$ do blobs follow pre-existing channel?

$\Longrightarrow$ nonballistic motion?

$\Longrightarrow$ difference between bulk motion and pattern motion?

(Kellermann et al., 2004, Fig. 7)

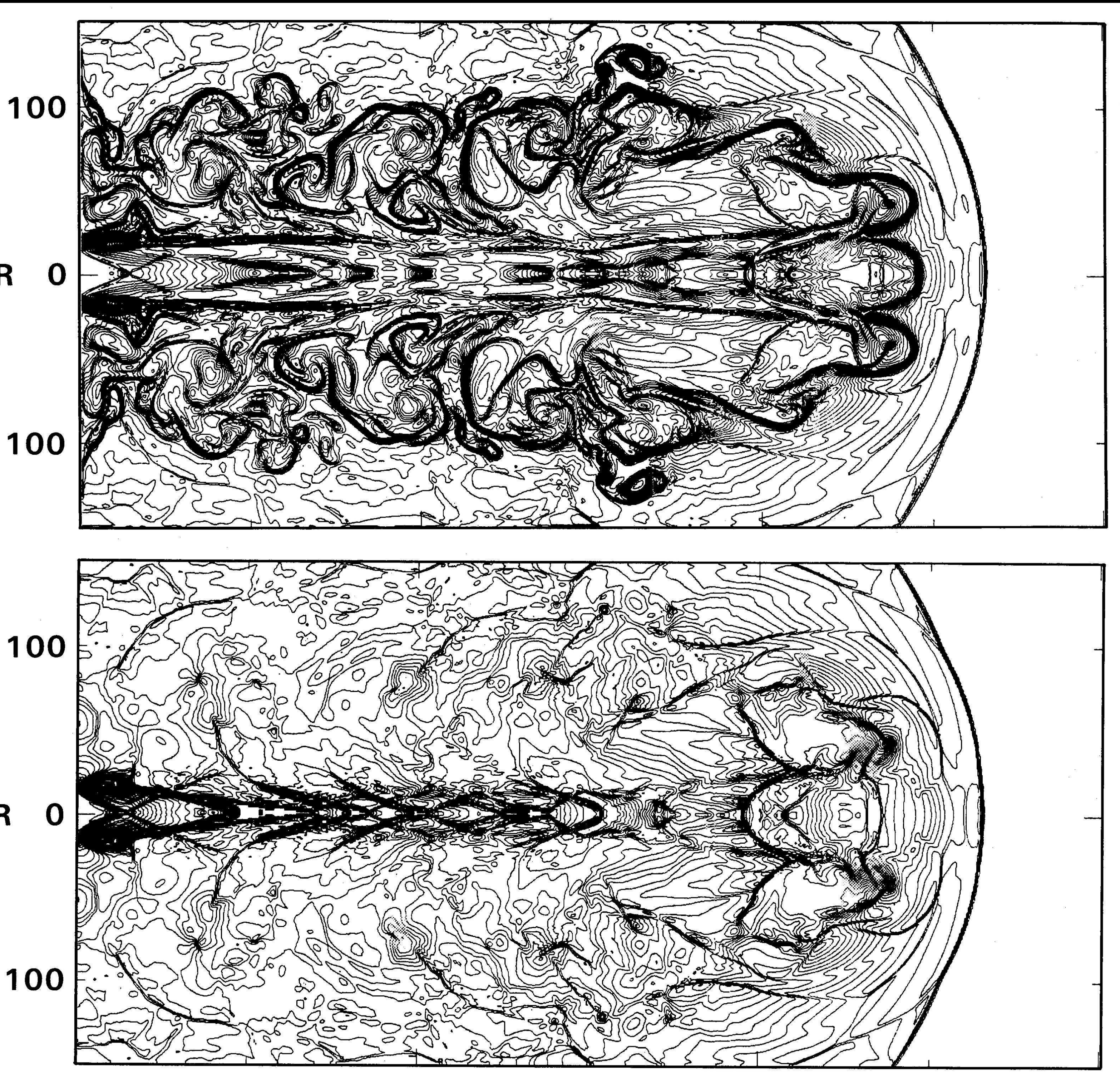

Jet propagation is very diffi cult hydrodynamics: generally solved numerically

Numerical simulation of a Mach=6 jet (Top: density, bottom: pressure Lind et al., 1989).

Turbulent structure due to Kelvin-Helmholtz instability (hydrodynamical instability in shear fbws)

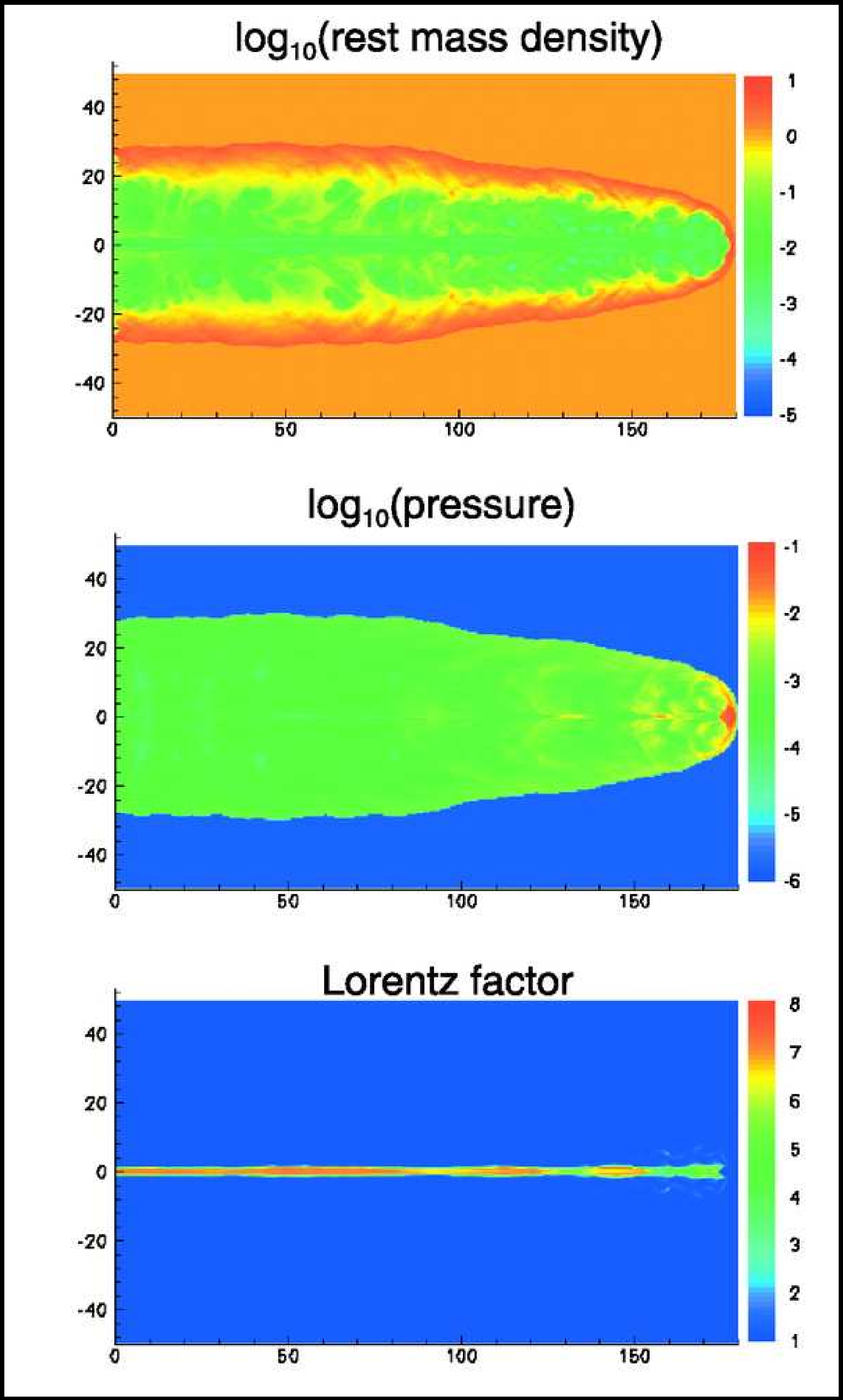

(Mizuta, Yamada & Takabe, 2004)

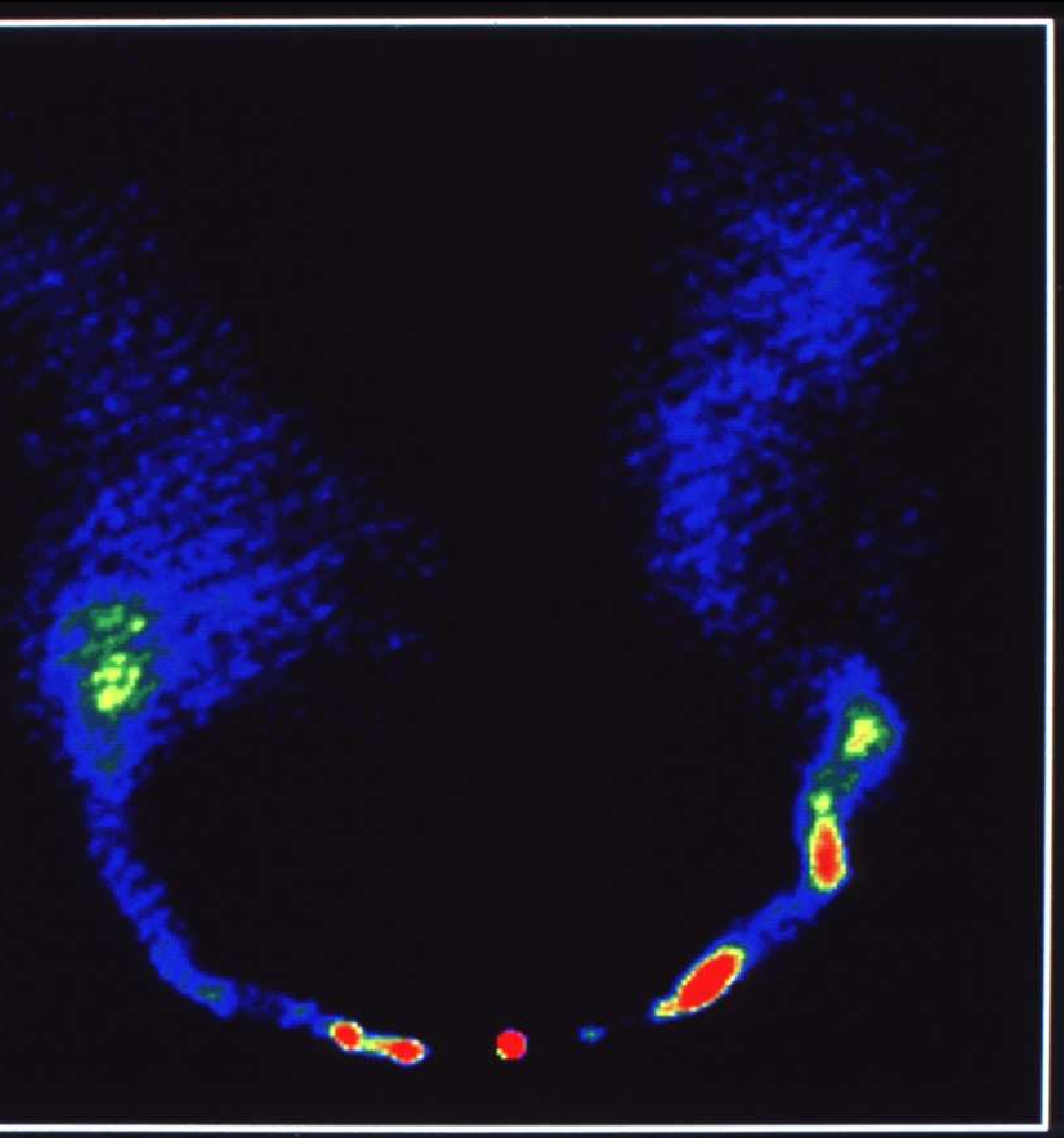

NGC 1265: radio galaxy in Perseus cluster, moving with $2000\,\mathrm{km\,s^{-1}}$ through intergalactic medium.

(NRAO/AUI; O'dea & Owen, 1986)

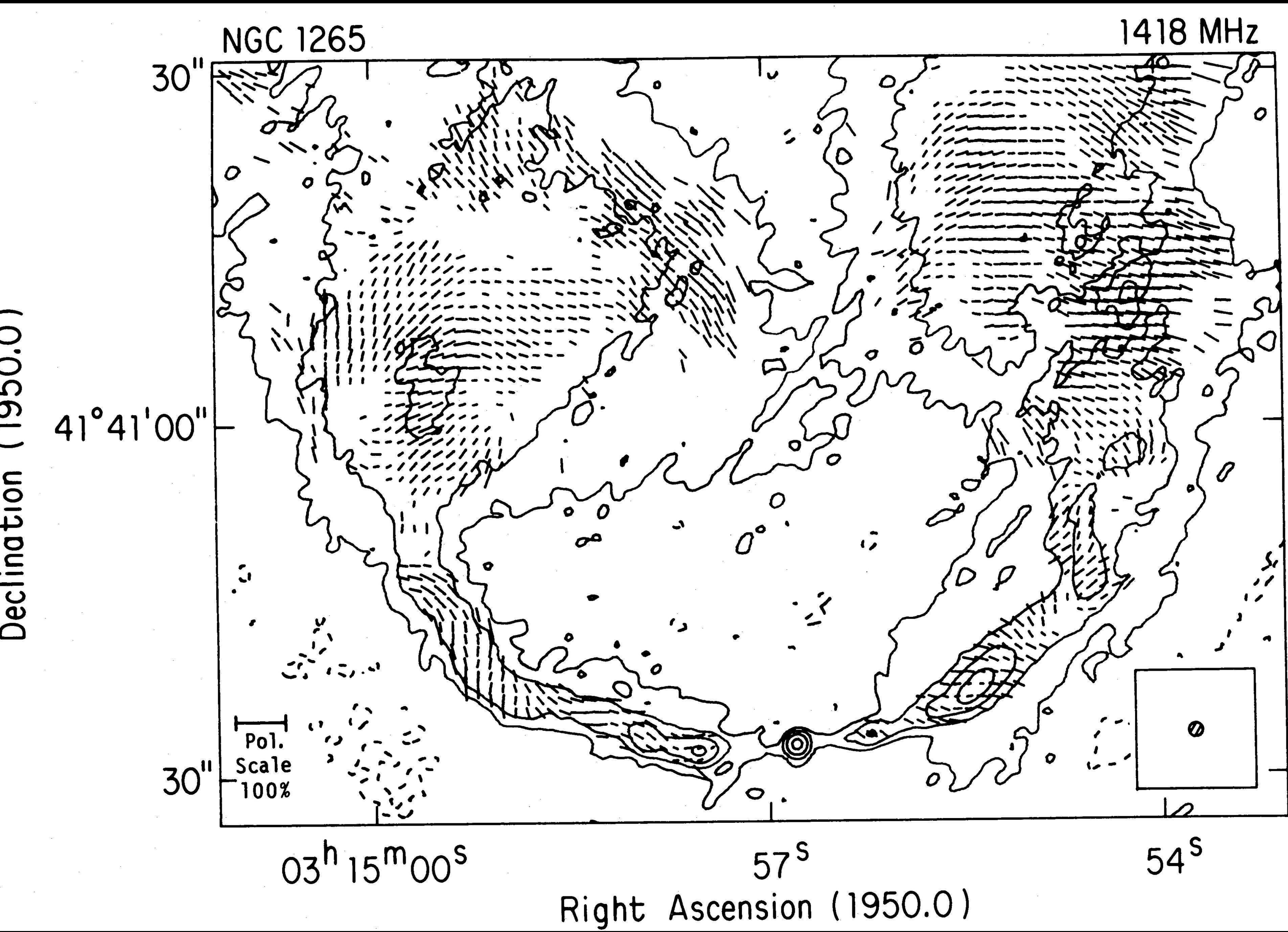

E-field structure of NGC 1265 (O'dea & Owen, 1986)

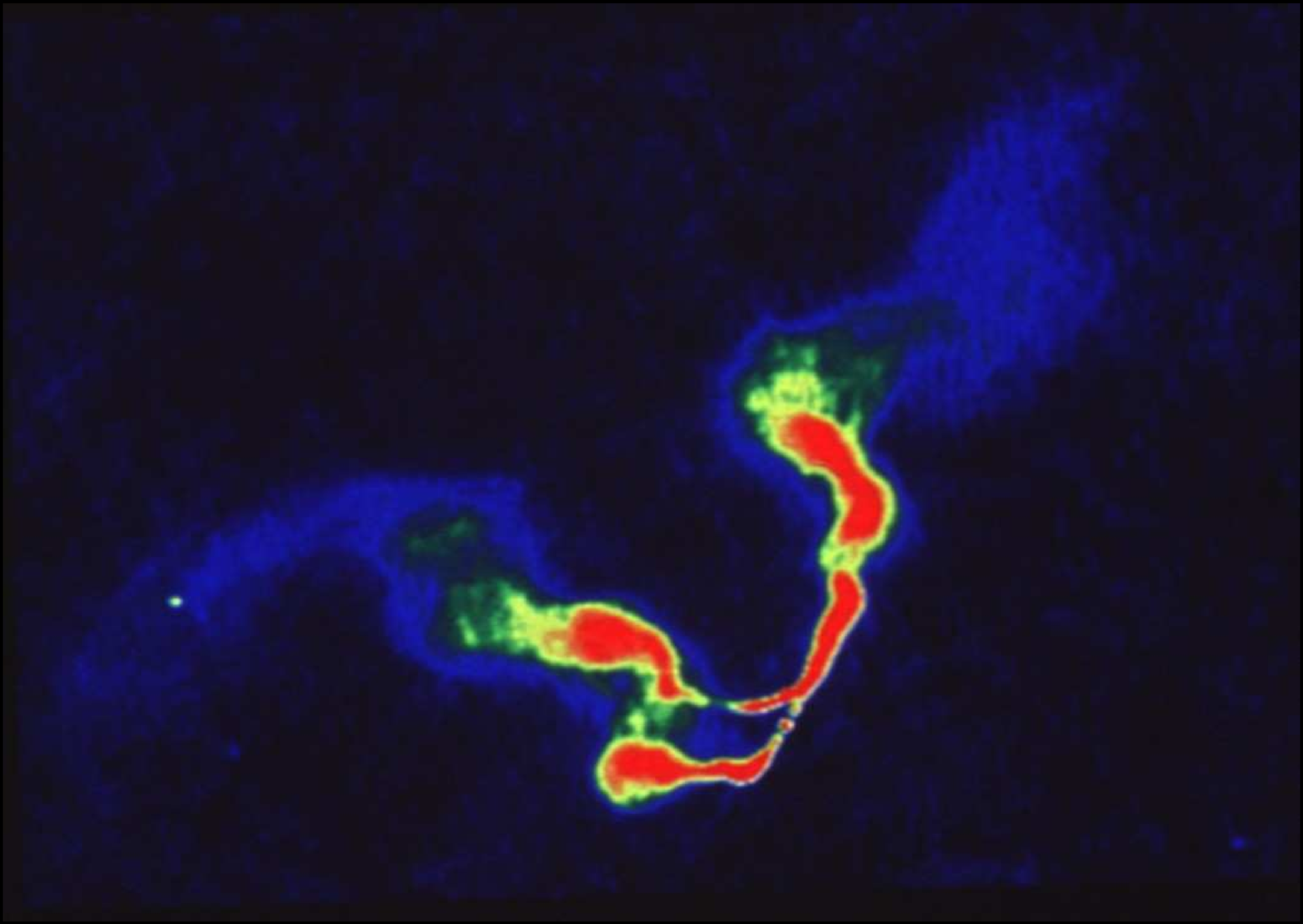

(NRAO/AUI/Owen et al.)

3C75 in Abell 400 at $\lambda = 20\,\mathrm{cm}$: twin radio jets from double core.

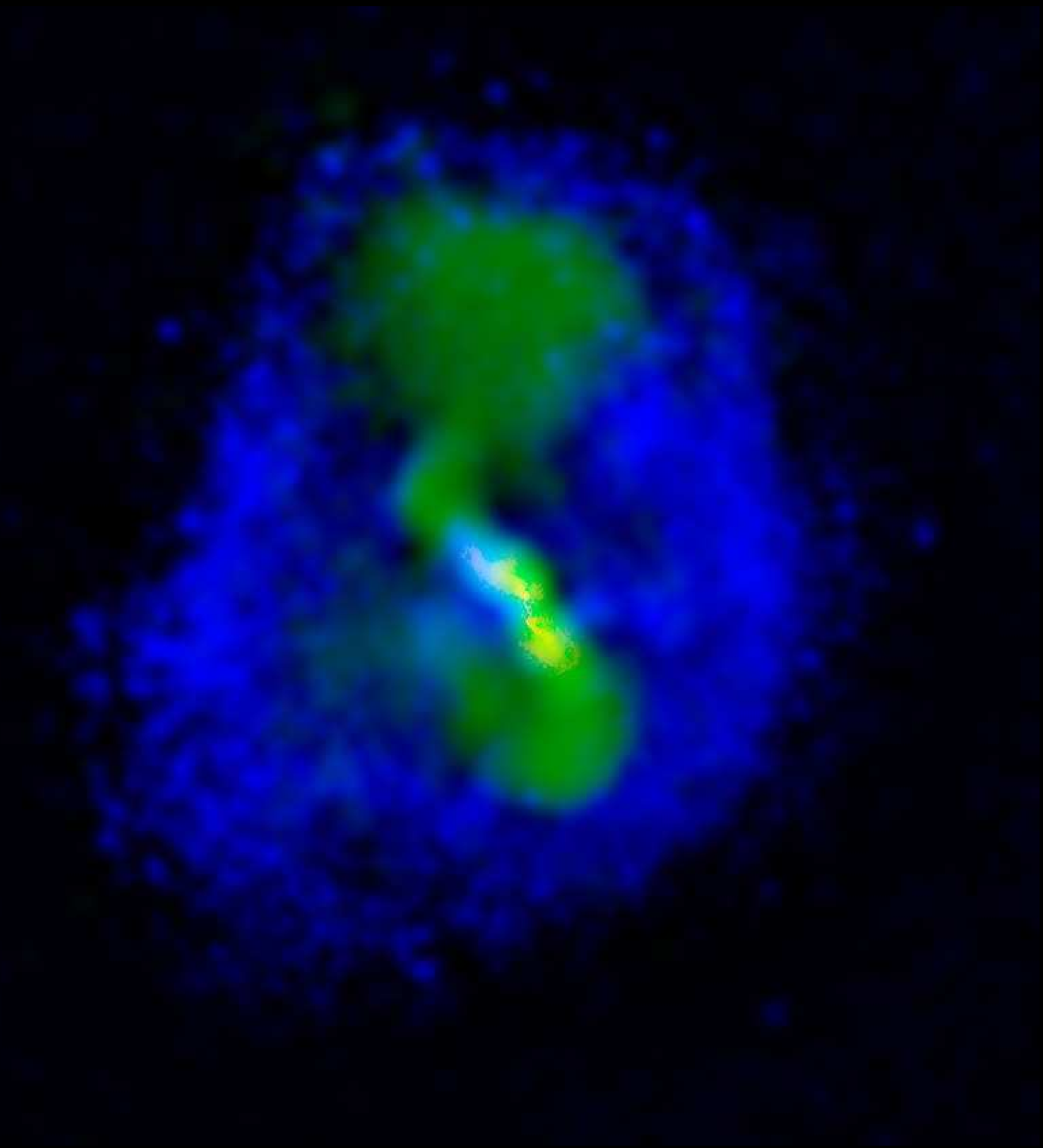

Hydra A: Multiple cavities drifting outwards through the intergalactic medium. Cavity system created in the past 200–500 Myears

green: radio, blue: X-rays, after subtracting elliptical β-model for gas distribution.

Size scale: outer cavities have diameters of 200 and 120 kpc.

(courtesy Mike Wise, UvA, astro-ph/0612100)

Formation of jet substructure / cavities in MHD simulations of a jet penetrating into a cluster gas

courtesy M. Brüggen (IUB) and UKAFF

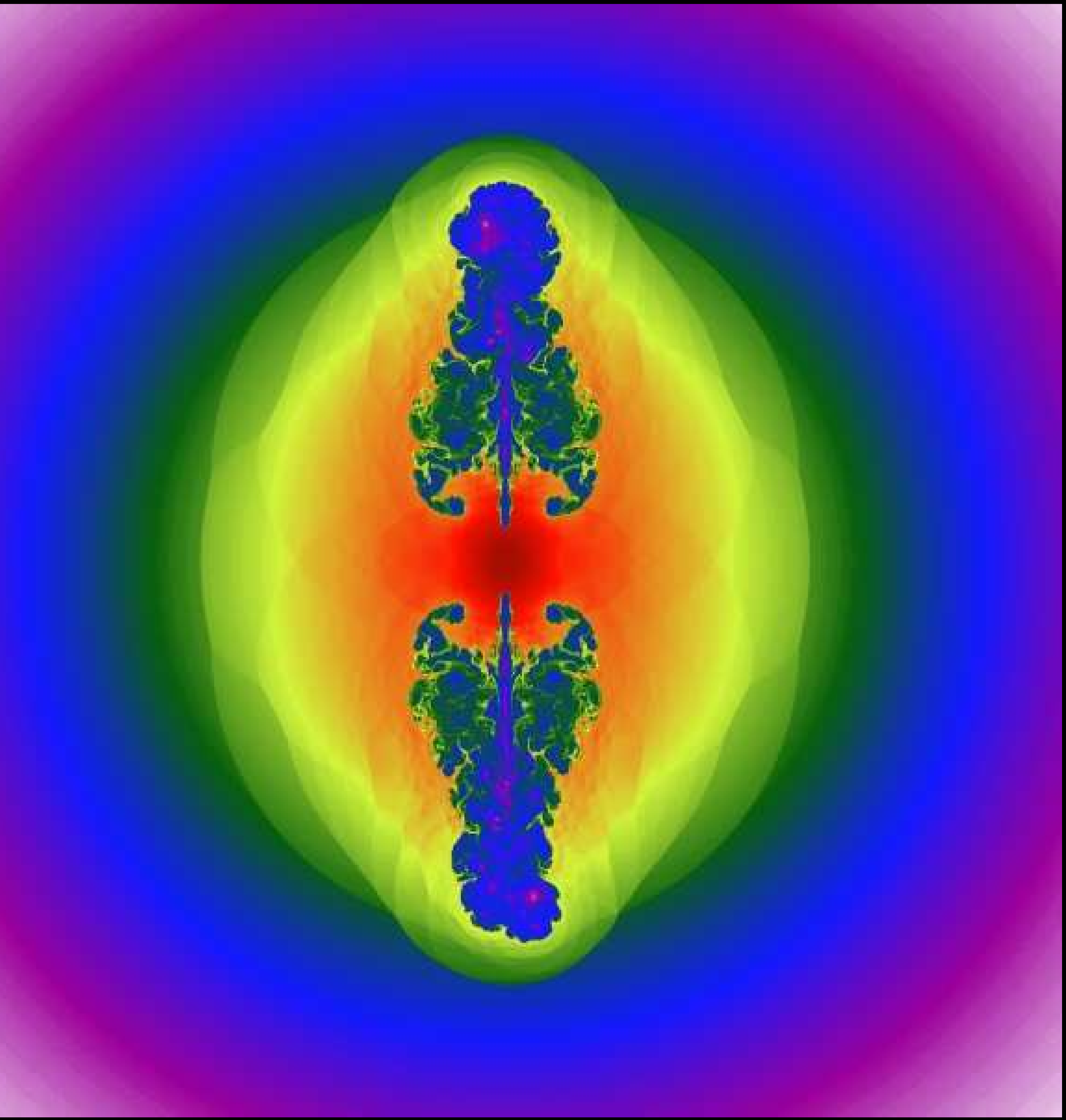

Global view of
jet-IGM-interaction and cavity
formation

courtesy M. Brüggen (IUB) and UKAFF

Movie: `jetmovies/brueggen_moviebig2.avi`

see Heinz et al., 2006, MNRAS

Jets and IGM, VII

Radio lobe physics:

Total energy content of lobe for a power law distribution of electrons, $n(E) = n_0 E^{-p}$:

$$U_\mathrm{e} = V \int_{E_1}^{E_2} n(E)\, E\, dE = \frac{V n_0}{2-p} \left(E_2^{2-p} - E_1^{2-p} \right) \tag{10.52}$$

Integrating over the synchrotron spectrum (Eq. (10.26)) gives the total synchrotron luminosity produced by this electron population:

$$L = \frac{4\sigma_\mathrm{T} U_B V n_0}{3 m_\mathrm{e}^2 c^4} \left(\frac{E_2^{3-p} - E_1^{3-p}}{3-p} \right) \tag{10.53}$$

Using the characteristic frequency

$$\omega_\mathrm{c} = \gamma^2 \omega_\mathrm{L} = \frac{eB}{m_\mathrm{e} c} \left(\frac{E}{m_\mathrm{e} c^2} \right)^2 \tag{10.18}$$

E_1 and E_2 can be expressed in terms of the frequency band over which the power law is observed, ν_1, ν_2. After some messy calculation one obtains:

$$\frac{U_\mathrm{e}}{L} = \frac{A}{B^{3/2}} \tag{10.54}$$

where A is some constant.

Jets and IGM, VIII

The total kinetic energy in particles is

$$U_{\text{particles}} = aU_{\text{e}} = aAB^{-3/2}L \tag{10.55}$$

where $a > 1$ (since there are other particles than electrons in the lobe).

Therefore the total energy of the radio lobe is

$$U_{\text{tot}} = U_{\text{particles}} + U_B = \frac{aAL}{B^{3/2}} + \frac{VB^2}{8\pi} \tag{10.56}$$

The minimum of U_{tot} is reached for

$$B_{\text{min}} = \left(\frac{6\pi aAL}{V}\right)^{2/7} \tag{10.57}$$

while the equipartition B-field, for which $U_{\text{particles}} = U_B$ is

$$B_{\text{eq}} = \left(\frac{8\pi aAL}{V}\right)^{2/7} \tag{10.58}$$

Since the total energy for equipartition is $1.01U_{\text{min}}$, one often assumes synchrotron sources are in equipartition.

First noticed by Burbidge (1959).

Jets and IGM, IX

Radio lobes:

- Typical luminosity is a few times $L = 10^{44}\,\mathrm{erg\,s^{-1}}$
- Typical B-fields are $\sim 10^{-4}\,\mathrm{G}$

Assuming equipartition: typical energy content of a radio lobe: $E \sim 10^{60}\,\mathrm{erg}$

corresponding to 10^7 supernovae

$\Longrightarrow$ lobe lifetime $t \sim E/L \sim 10^8\,\mathrm{yr}$

$\Longrightarrow$ jets and lobes are rather long lived phenomena

Equipartition holds only approximately true for jets and lobes (see, e.g., Heinz & Begelman 1997).

Jet Formation

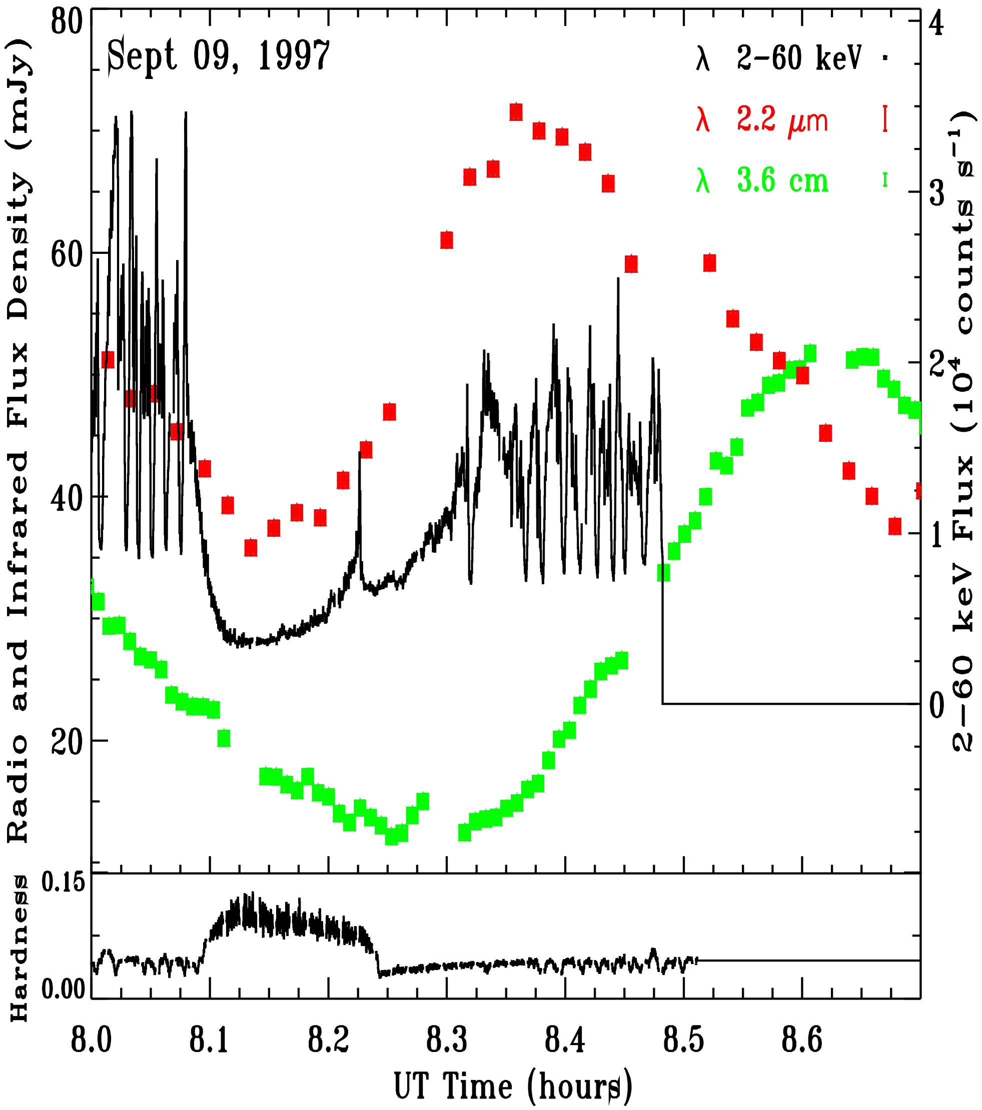

Dynamics of jet formation are better studied in Galactic black holes with jets ("microquasars") because of shorter timescales.

Find clear X-ray–radio correlation (similar also seen in some AGN such as 3C120)

$\Longrightarrow$ "universal disk-jet-connection"

(GRS 1915+105; Mirabel et al., 1998)

Jet Formation

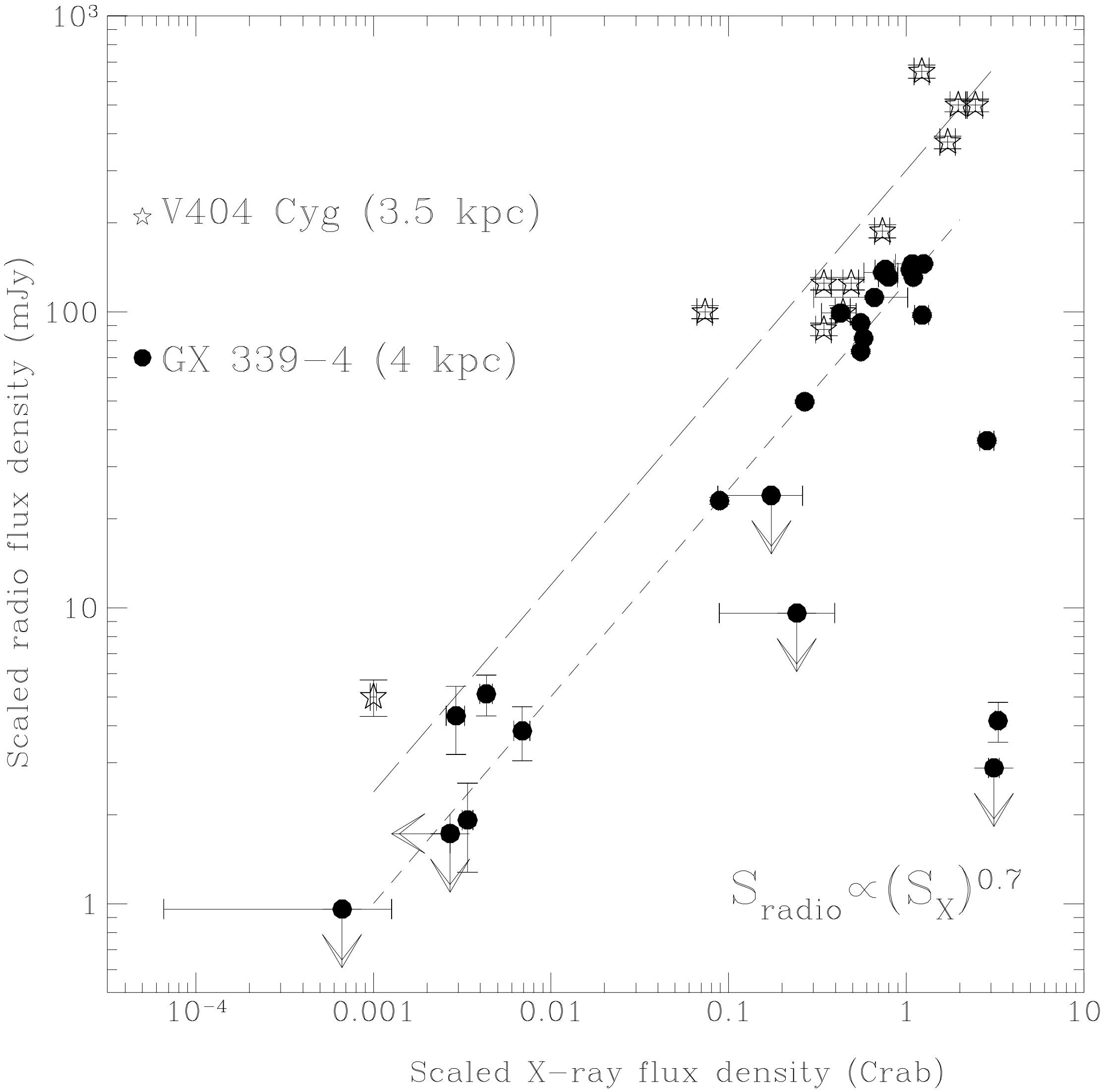

X-ray binaries: $S_{\text{radio}} \propto S_X^{0.7}$

$\Longrightarrow$ Radio and X-ray fluxes are correlated: evidence for interaction between disk and jet!

(Gallo, Fender & Pooley, 2003)

movie time: `jetmovies/agn_xray_020505_11_640x480_95pc`

Marscher et al. (2002): 3C120: X-ray dips followed by radio ejection events

$\Longrightarrow$ jets and accretion disk are related.

Jet Formation

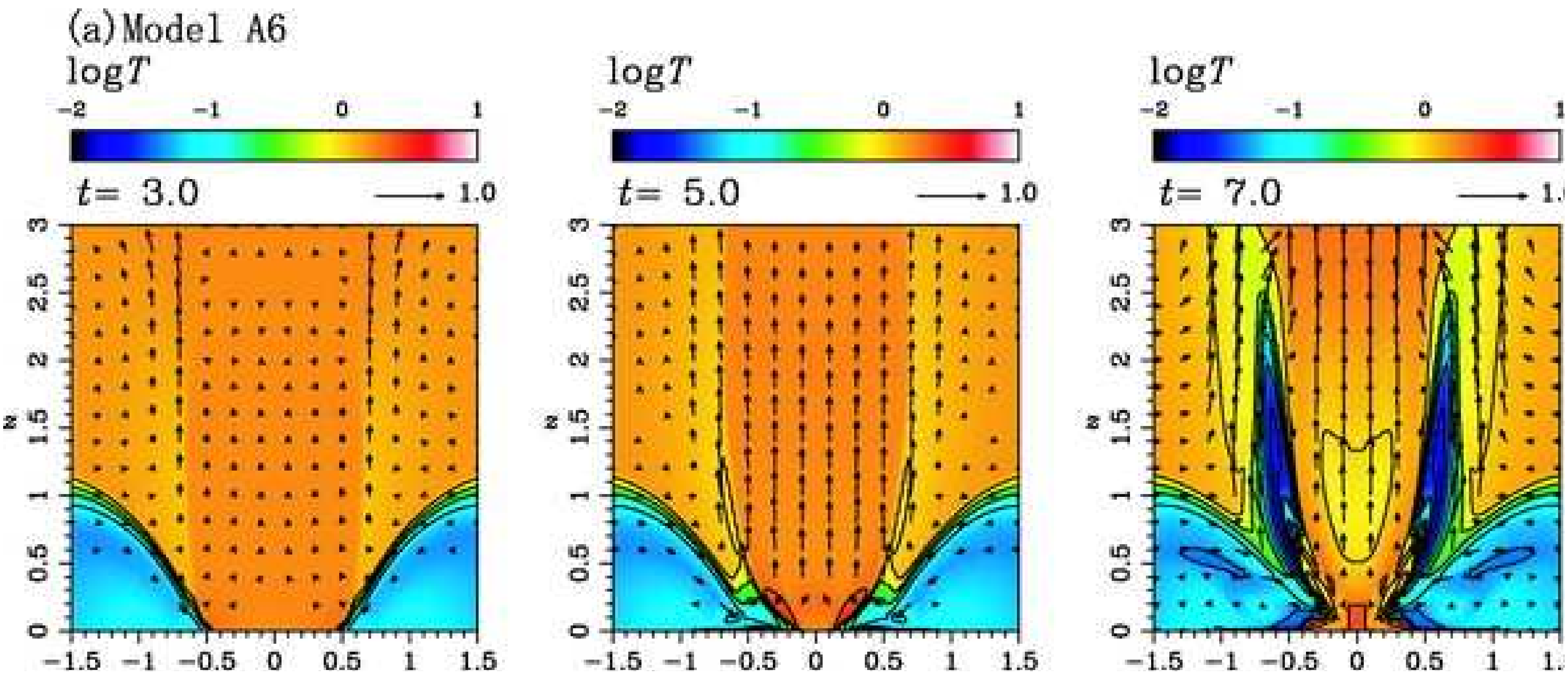

Evolution of a newly launched jet (Kigure & Shibata, 2005)

To study jet confinement and propagation: use magnetohydrodynamical simulations

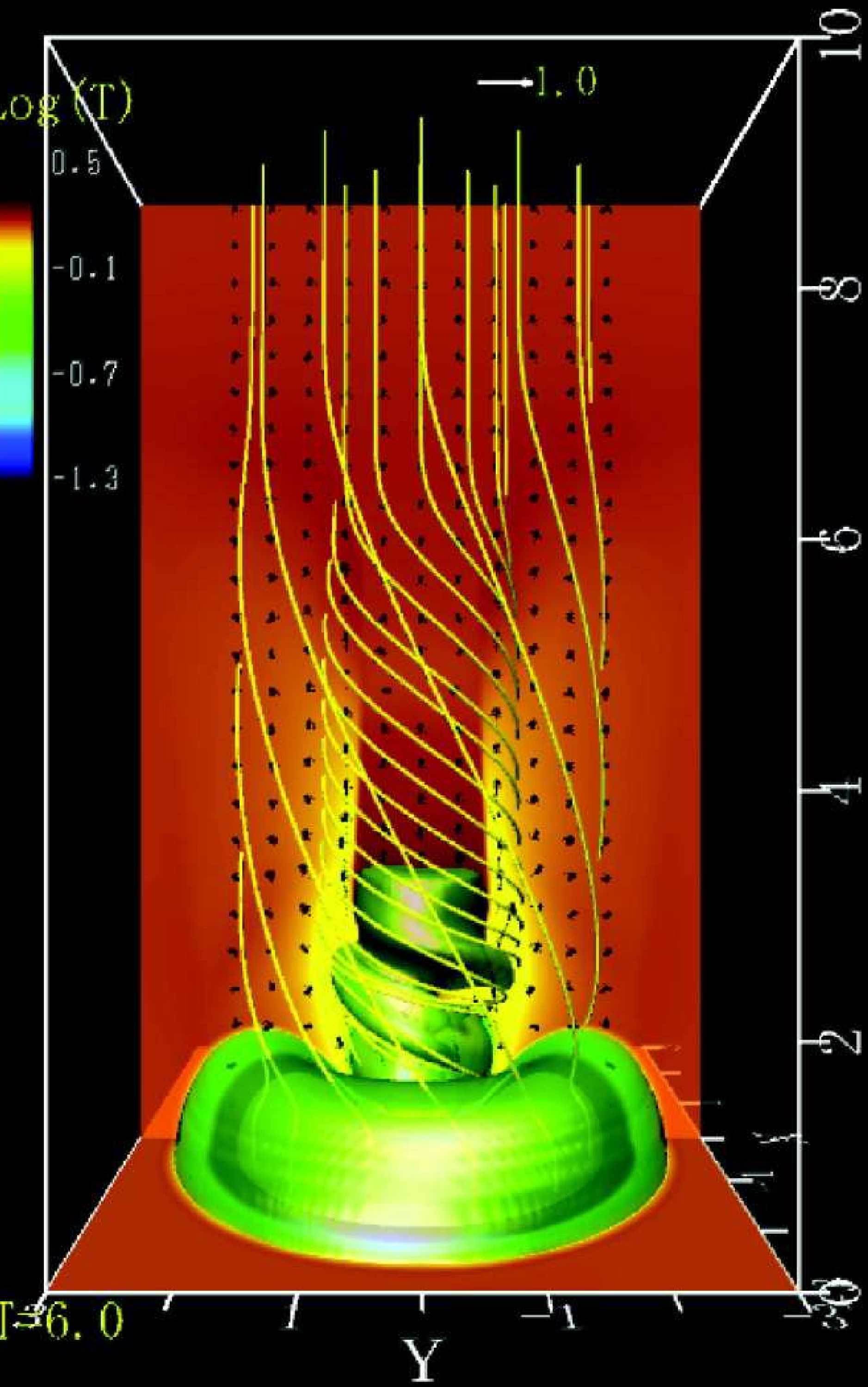

Temperature profile and B-field configuration of a MHD-jet

Movie: `jetmovies/d155mvj.avi`: Time evolution of B-fi eld and density close to a BH (Matsumoto&Machida).

(Kigure & Shibata, 2005, Fig. 6)

Jet Formation

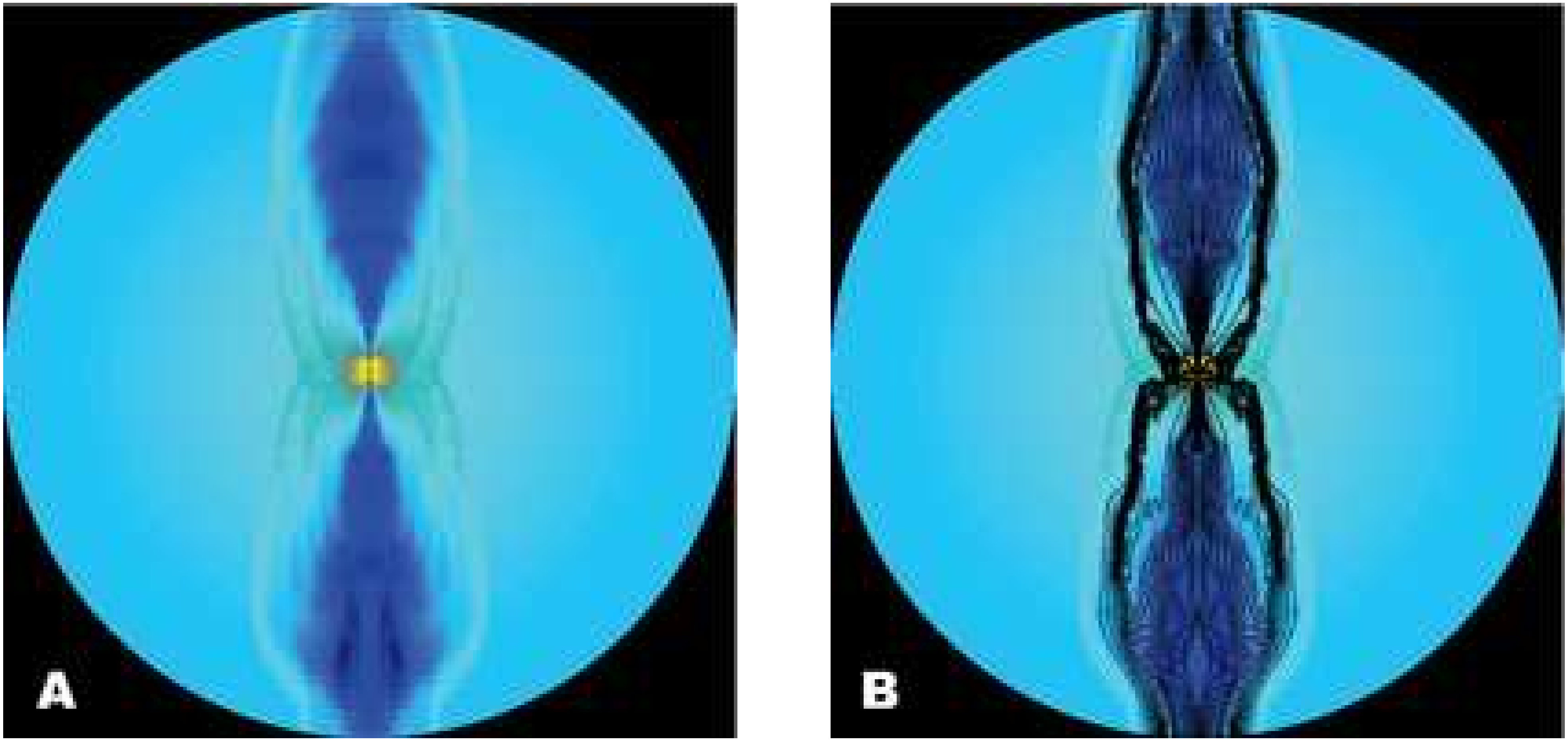

(McKinney, 2006, Fig. 1)

$\log\rho$ (left) and $\log\rho$ and B for a jet launched via a disk.
Outer radius is $10^4 GM/c^2$.

Jet Formation

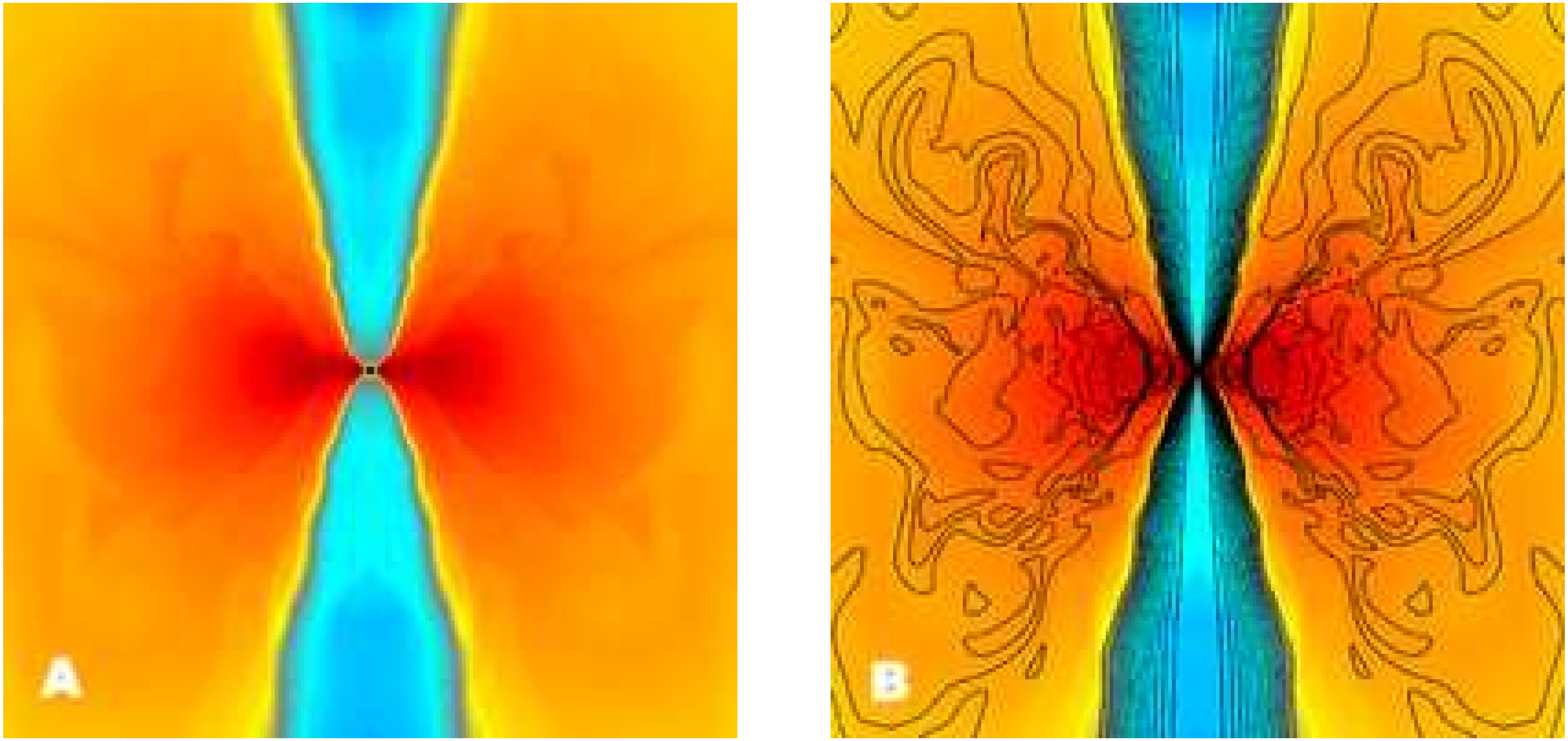

(McKinney, 2006, Fig. 2)

$\log \rho$ (left) and $\log \rho$ and B for a jet launched via a disk.
Outer radius is $10^2 GM/c^2$.

Jet Formation

Movie time:

- `diskmovies/rho3.mpg`: jet simulation out to $40GM/c^2$ (McKinney)
- `diskmovies/rout400new.lrho.3.mpg`: jet simulation out to $400GM/c^2$ (McKinney)

Blumenthal, G. R., & Gould, R. J., 1970, Rev. Mod. Phys., 42, 237

Burbidge, G. R., 1959, ApJ, 129, 849

Gallo, E., Fender, R. P., & Pooley, G. G., 2003, MNRAS, 344, 60

Ginzburg, V. L., & Syrovatskii, S. I., 1965, Ann. Rev. Astron. Astrophys., 3, 297

Ginzburg, V. L., & Syrovatskii, S. I., 1969, Ann. Rev. Astron. Astrophys., 7, 375

Heinz, S., & Begelman, M. C., 1997, ApJ, 490, 653

Kellermann, K. I., et al., 2004, ApJ, 609, 539

Kigure, H., & Shibata, K., 2005, ApJ, 634, 879

Killeen, N. E. B., Bicknell, G. V., & Ekers, R. D., 1986, ApJ, 302, 306

Laing, R. A., & Bridle, A. H., 1987, MNRAS, 228, 557

Lind, K. R., Payne, D. G., Meier, D. L., & Blandford, R. D., 1989, ApJ, 344, 89

Marscher, A. P., Jorstad, S. G., Gómez, J.-L., Aller, M. F., Teräsranta, H., Lister, M. L., & Stirling, A. M., 2002, Nature, 417, 625

McKinney, J. C., 2006, MNRAS, 368, 1561

Mirabel, I. F., Dhawan, V., Chaty, S., Rodríguez, L. F., Martí, J., Robinson, C. R., Swank, J., & Geballe, T. R., 1998, A&A, 330, L9

Mizuta, A., Yamada, S., & Takabe, H., 2004, ApJ, 606, 804

O'dea, C. P., & Owen, F. N., 1986, ApJ, 301, 841

Perley, R. A., Bridle, A. H., & Willis, A. G., 1984, ApJS, 54, 291

Perlman, E. S., Biretta, J. A., Sparks, W. B., Macchetto, F. D., & Leahy, J. P., 2002, New Astronomy Review, 46, 399

Reynolds, S. P., 1982, ApJ, 256, 13

Rybicki, G. B., & Lightman, A. P., 1979, Radiative Processes in Astrophysics, (New York: Wiley)